AD-A034 187 AIR FORCE ROCKET PROPULSION LAB EDWARDS AFB CALIF F/G 21/8.2
STRUCTURAL COMPUTER CODE EVALUATION. VOLUME II.(U)
NOV 76 J H HILDRETH
UNCLASSIFIED AFRPL-TR-76-68-VOL-2 NL

1 OF 1
AD
A034187

END
DATE
FILMED
2-77

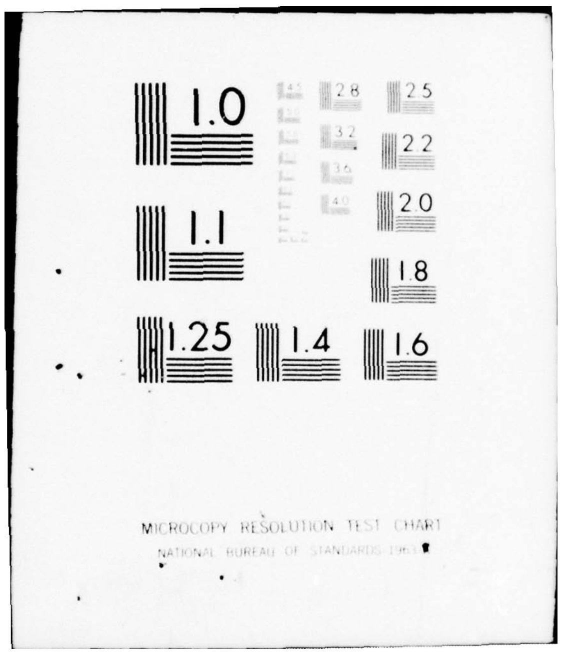
1.0
1.1
1.25
1.4
1.6
1.8
2.0
2.2
2.5
2.8
3.2
3.6
4.0
MICROCOPY RESOLUTION TEST CHART
NATIONAL BUREAU OF STANDARDS-1963-A

12

B.S.

AFRPL-TR-76-68

STRUCTURAL COMPUTER CODE EVALUATION

FINAL REPORT VOLUME 2

LT. JOSEPH H. HILDRETH

NOVEMBER 1976

APPROVED FOR PUBLIC RELEASE
DISTRIBUTION UNLIMITED

AIR FORCE ROCKET PROPULSION LABORATORY
DIRECTOR OF SCIENCE AND TECHNOLOGY
AIR FORCE SYSTEMS COMMAND
EDWARDS AFB, CALIFORNIA 93523

NOTICES

FOREWORD

The work described in this report was performed during fiscal year 1976. It was funded jointly by the Air Force Rocket Propulsion Laboratory under Job Order No. 305910MB and by Strategic Systems Project Office under Naval Weapons Center Job Order No. 14571110. This effort was part of a task performed jointly by AFRPL and NWC to evaluate structural computer codes for analysis of rocket nozzles.

The work was documented in two volumes. Volume I contains a final report and summary of computer codes evaluated in this study; this work was performed mainly at NWC. Volume II contains results from solving several sample problems using selected computer codes; this work was performed mainly at AFRPL.

Joseph H. Hildreth

JOSEPH H. HILDRETH, 1Lt, USAF
Project Engineer

John G. Dean

JOHN G. DEAN, Major, USAF
Chief, Design & Analysis Section

FOR THE COMMANDER

Charles R. Cooke

CHARLES R. COOKE
~~Director~~, Solid Rocket Division

UNCLASSIFIED

SECURITY CLASSIFICATION OF THIS PAGE (When Data Entered)

14

REPORT DOCUMENTATION PAGE

READ INSTRUCTIONS BEFORE COMPLETING FORM

1. REPORT NUMBER
AFRPL-TR-76-68 — Vol - 2

2. GOVT ACCESSION NO.

3. RECIPIENT'S CATALOG NUMBER
9

4. TITLE (and Subtitle)
6
STRUCTURAL COMPUTER CODE EVALUATION.
Vol II
Volume II.

5. TYPE OF REPORT & PERIOD COVERED
Final Report .
Jul[redacted] [redacted]75 — Aug[redacted] [redacted]76,
(6)

6. PERFORMING ORG. REPORT NUMBER

7. AUTHOR(s)
10
Joseph H. Hildreth

8. CONTRACT OR GRANT NUMBER(s)

9. PERFORMING ORGANIZATION NAME AND ADDRESS
Air Force Rocket Propulsion Laboratory/AFSC
Edwards AFB, California 93523

10. PROGRAM ELEMENT, PROJECT, TASK AREA & WORK UNIT NUMBERS
JON 305910MB

11. CONTROLLING OFFICE NAME AND ADDRESS

12. REPORT DATE
11
Nove[redacted]r [redacted]76

13. NUMBER OF PAGES
71

14. MONITORING AGENCY NAME & ADDRESS(if different from Controlling Office)
12
76p.

15. SECURITY CLASS. (of this report)
UNCLASSIFIED

15a. DECLASSIFICATION/DOWNGRADING SCHEDULE

16. DISTRIBUTION STATEMENT (of this Report)

APPROVED FOR PUBLIC RELEASE; DISTRIBUTION UNLIMITED

17. DISTRIBUTION STATEMENT (of the abstract entered in Block 20, if different from Report)

16 3059 17 10

18. SUPPLEMENTARY NOTES

19. KEY WORDS (Continue on reverse side if necessary and identify by block number)

Structural Computer Codes	TEXGAP
Finite Element	NOZZLE DESIGN
NEPSAP	Nonlinear Structural Analysis
NONSAP	Linear-Elastic Structural Analysis
SAAS	Elastic-Plastic Structural Analysis

20. ABSTRACT (Continue on reverse side if necessary and identify by block number)

This document is Volume 2 of the final report on the evaluation of current structural computer codes. This program was a joint effort between the Naval Weapons Center and the Air Force Rocket Propulsion Lab to determine the capabilities of current structural codes versus the capabilities needed to analyze state of the art solid rocket nozzles. The project was intended to be a first step of a continuing evaluation process as newer codes become available. The work consisted of a survey of available structural codes, an

DD FORM 1 JAN 73 1473 EDITION OF 1 NOV 65 IS OBSOLETE

UNCLASSIFIED

SECURITY CLASSIFICATION OF THIS PAGE (When Data Entered)

307720

YB

evaluation of their theoretical capabilities, installation of 4 codes on RPL's computer, and 4 analyses and results, and conclusions of the program are presented in this volume.

CONTENTS

ILLUSTRATIONS

LIST OF TABLES

LIST OF TABLES (Cont.)

SECTION I

INTRODUCTION

The art of performing nozzle structural analysis for solid rockets has become increasingly more difficult in the past several years. The difficulty has occurred due to the introduction of exotic carbon materials to withstand increasing hostile nozzle environments. These newer materials have generated four problem areas for the nozzle community; a lack of accurate material property data, a lack of adequate failure criteria, difficulty with consistent material reproducibility, and a lack of adequate models in current computer codes to analyze these materials.

Substantial money and effort has been and continues to be spent by the Naval Weapons Center (NWC) and the Air Force Rocket Propulsion Laboratory (AFRPL) addressing the problems of material properties, failure criteria, and reproducibility. However, little formal effort has been directed toward eliminating the problems with state-of-the-art computer codes relative to the newer materials. This program is a first step toward the solution of this problem.

More than anything else, this program confirmed two accepted facts: 1. There is not yet available a code which meets all of the needs of the nozzle community, 2. The present codes perform equally well for linear-elastic analysis which, unfortunately, is the only type of analysis this program had time to investigate. One significant item was discovered. The core requirements and runtimes for a general 3-D code running in the axisymmetric mode, in this case NEPSAP, were not significantly greater than SAAS III for analyzing 2-D axisymmetric problems. This means that the cost of using a 3-D code is not prohibitive for solving geometrically simpler problems.

Volume I of this report presents a summary of nonlinear analysis, a discussion of the features now needed for stress analysis, and summaries of the codes which were surveyed and evaluated. This volume will present the installation of the 4 codes which were selected for running, the analyses which were performed with these codes, the data and results of the analyses, and conclusions.

SECTION II

INSTALLATION AND MODIFICATIONS

Four codes were chosen and installed on the AFRPL computer for further evaluation. All four codes required some modification for the purposes of this evaluation. Most of the modifications were to reduce the core requirements so that they would fit within the somewhat small allowable core size of the AFRPL computer ($140,000_8$* locations or approximately 49,000 decimal locations).

The four codes installed for this program were SAAS III, TEXGAP, NONSAP, and NEPSAP. Each of the codes will be discussed separately below concerning version of code used, modifications, installation problems and core required for execution.

The SAAS III code which was used for this program was already operational at the AFRPL. The code was obtained from Aerospace Corporation in April of 1973. Since that time the code had undergone several modifications to reduce the required core for execution. Another modification changed the method for interpolating the nodal temperatures. This modification changed the scheme by which the input temperature points were chosen for interpolation so that problems encountered due to high thermal gradients were eliminated. Finally, specifically for this project, a time log was added to output the execution times for various segments of the code. In this configuration SAAS III loads in $125,000_8$ locations.

The TEXGAP code was also operational before the start of the program. This code was developed by Dr. Eric Becker and Dr. Robert Dunham at the University of Texas at Austin under an AFRPL contract. The version used for this project incorporated modifications through Change 4 as released by Dr. Becker and Dr. Dunham. Only two additional minor changes were made for this program. The first allowed a two card input for orthotropic material properties and the second was the installation of a time log to output execution times for various segments of the program. TEXGAP loads in $106,000_8$ locations.

NONSAP was obtained from the University of California at Berkley in June of 1975. The only change made in this code was the removal of the RETURN statements in the secondary level overlay programs. NONSAP loads in $131,000_8$ locations.

*Octal numbers are designated by the subscripted 8.

NEPSAP was obtained from the Aerospace Structures Information and Analysis Center (ASIAC) at Wright-Patterson AFB, Ohio through the Naval Weapons Center. This version was set up for the CDC system, but it also contained all the required statements for the UNIVAC system. The UNIVAC statements had been essentially removed by making them comment statements.

NEPSAP required substantial work to make it operational. The biggest problem was to reduce its size so the code would load into the AFRPL system. To accomplish this, all of the I/O buffer lengths were reduced to 512 locations, and the blank common length was reduced from 15000 to 12900. This allowed the code to load in $127,000_8$ locations. Several other modifications were also made. All of overlay 3 was removed. This overlay set up the instructions for the post processing plot program which the AFRPL does not have. The time log subroutines had to be rewritten to make them work on the AFRPL CDC 6400 Computer. In addition several subroutines still contained active statements for the UNIVAC system plus many other statements not required by the CDC system which had to be removed.

During the course of the program it was discovered that NEPSAP did not have an orthotropic material model for the 2-D axisymmetric element. At that time a subroutine from SAP IV was added to NEPSAP which partially fixed the problem. The fix was partial because it affected only the displacements and strains. The amount of work needed to make the orthotropic model work for the stresses, due to the nature of the solution process, was determined to be outside the scope of this project.

SECTION III

ANALYSES

PROBLEM DESCRIPTIONS

The problems chosen for analysis with each of the codes installed were presented in Volume I of this report. They are repeated here for convenience.

Three of the four problems are problems which were sent to all solid propellant contractors by the JANNAF Structures and Mechanical Behavior Working Group and the Operational Serviceability Working Group to get a comparison of the finite element capabilities of the various contractors. These problems were chosen for three reasons: (1) they are practical problems, (2) the results published in the Thiokol report* to the JANNAF committees provides an additional data point for comparison, (3) the JANNAF committees and contractors are familiar with these problems which will aid in their assessment of the results presented in this report. Results from the Thiokol analyses appear in this report in two cases for problem number 3.

For this program, two of the JANNAF problems were run for two values of Poisson's Ratio, 0.4999 and 0.30. This test was done so that the nonreformulated finite elements used in SAAS III, NONSAP, and NEPSAP would not be penalized for using values of Poisson's Ratios close to 0.50. Also for problem number 2, sphere under internal pressure, the radius was not allowed to go to zero, because a zero radius causes severe problems for finite element solutions.

Problem number 1 is a plane-stress cylinder subjected to internal pressure only. The grid and boundary conditions which were used for all codes are shown in Figure 1.

The other input parameters are:

Internal Pressure = 100 psi
$E = 1000$ psi
$\nu = .4999$

Problem number 2 is an internally pressurized sphere. The grid is basically the same as that used for problem number 1. The two minor differences are

*Anderson, G. P., and M. D. Black, "Finite Element Stress Analysis Check Problems," TWR-7808, Thiokol Chemical Corporation, Wasatch Division, 1974.

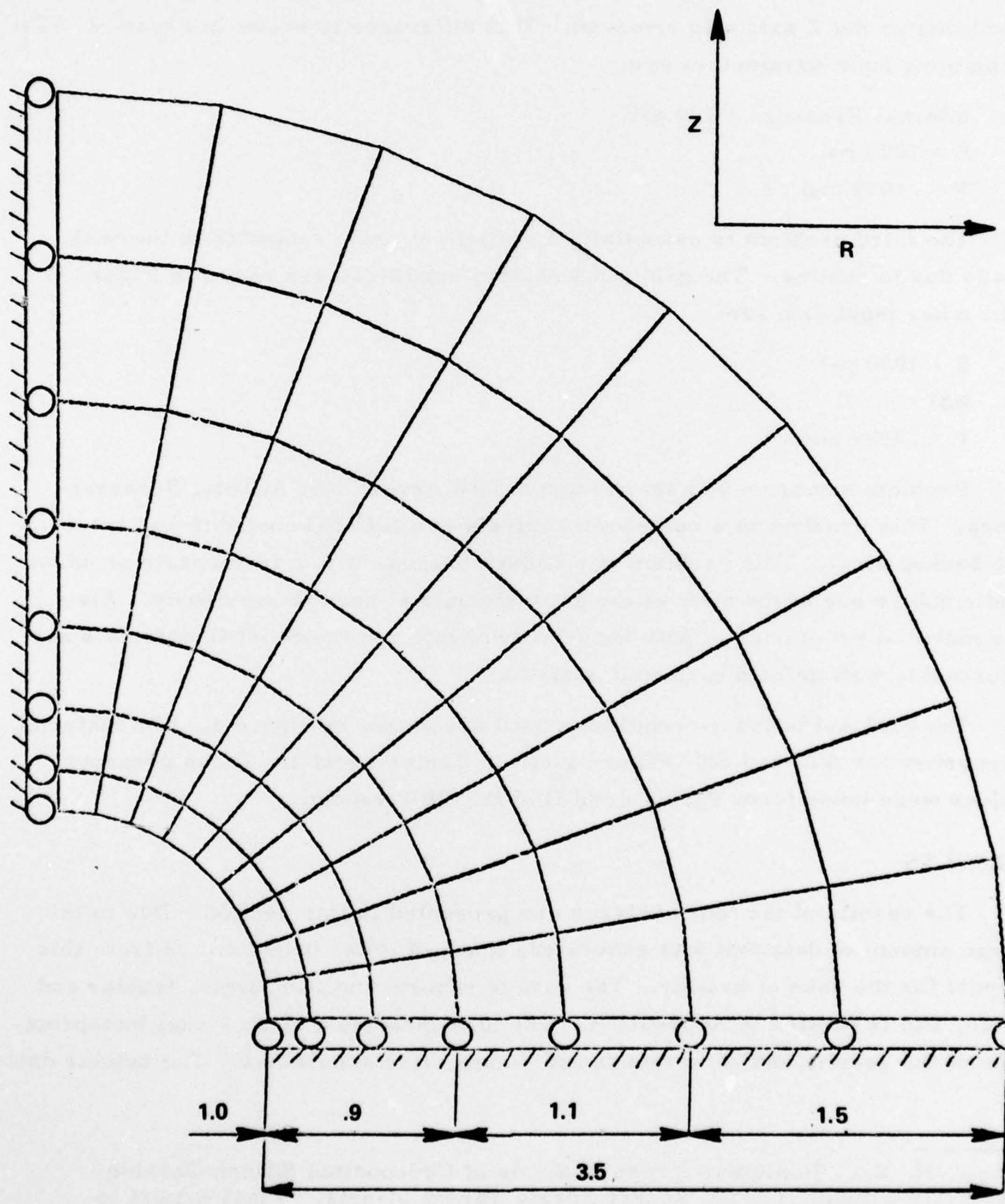

Figure 1. Grid for Problem Number 1

that the radius is not allowed to go to zero, and the radial displacement boundary condition on the Z axis was removed. This difference is shown in Figure 2. The remaining input parameters are:

Internal Pressure = 100 psi

E = 1000 psi

ν = .4999 and .3

The third problem is essentially a propellant grain subjected to thermal loads due to cooling. The grid and boundary conditions are shown in Figure 3. The other input data are:

E = 1000 psi

$\alpha\Delta T$ = - .01

ν = .4999 and .3

Problem number 4 was taken from a TRW report* for Atlantic Research Corp. This problem is a cool-down analysis of a SiC/PG coated throat insert (no backup ring). This problem was chosen because it is a true nozzle problem and employs one of the state of the art materials alluded to previously. Also the material properties of both the ATJ substrate and the SiC/PG materials are reasonably well defined to permit analysis.

The grid and boundary conditions used are shown in Figure 4. The material properties for ATJ and SiC/PG are given in Tables 1 and 2. These property values were taken from Tables I and II of the TRW report.

RESULTS

The results of the four analyses are presented in this section. Due to the large amount of data that was generated, much of it has been omitted from this report for the sake of brevity. The data is recorded in two forms, tabular and plots, and is located in Appendix A. The plots provide a clear visual interpretation of the results and show trends and comparitive accuracies. The tabular data

---

*King, K. R., "Nonlinear Stress Analysis of Codeposited Silicon Carbide-Pyrolytic Graphite Coated Rocket Nozzle Throat Inserts," Final Report to Atlantic Research Corporation, Cont. No. P.O. 78916, TRW Systems Group, Redondo Beach, Calif., Aug. 28, 1973.

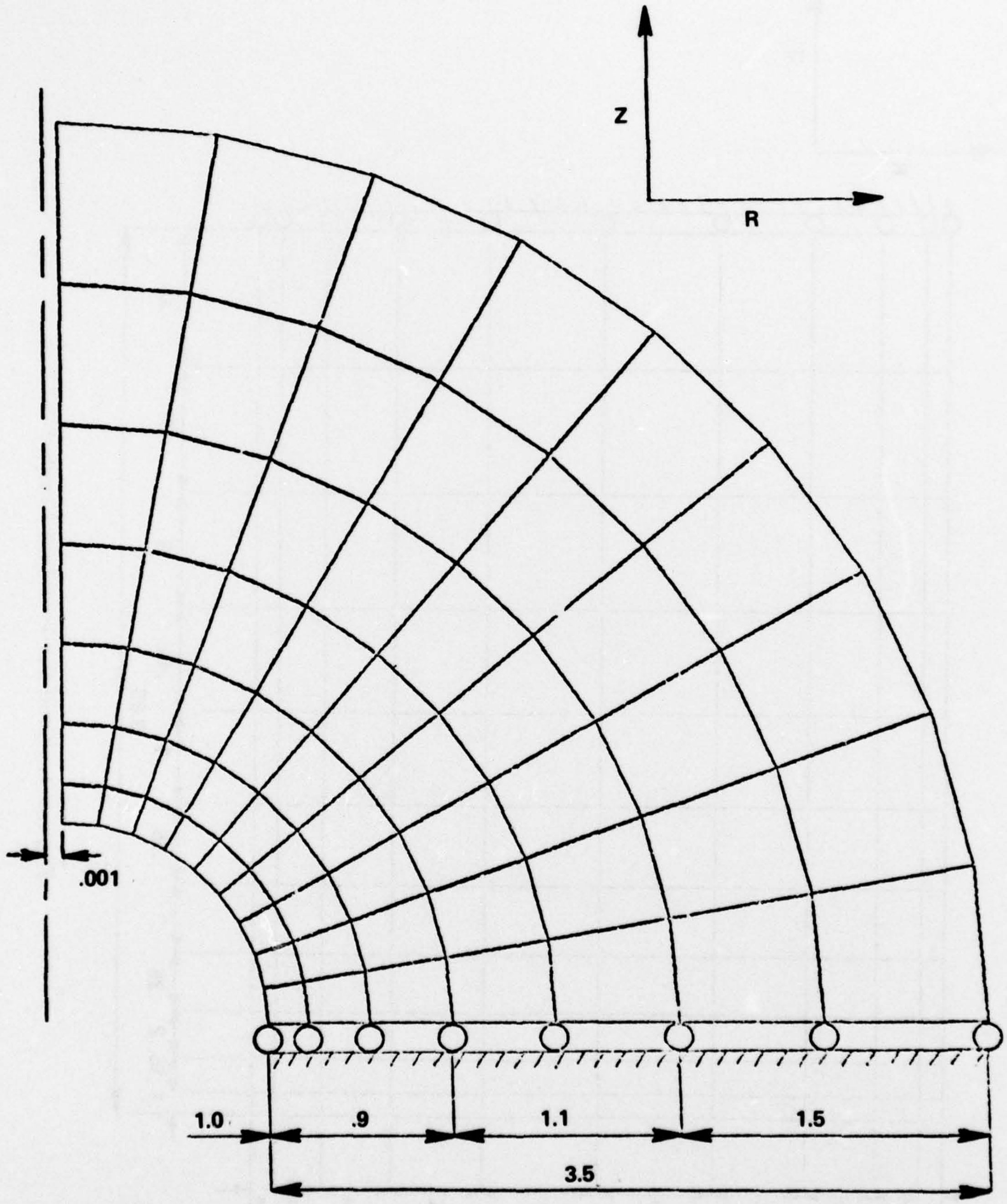

Figure 2. Grid for Problem Number 2

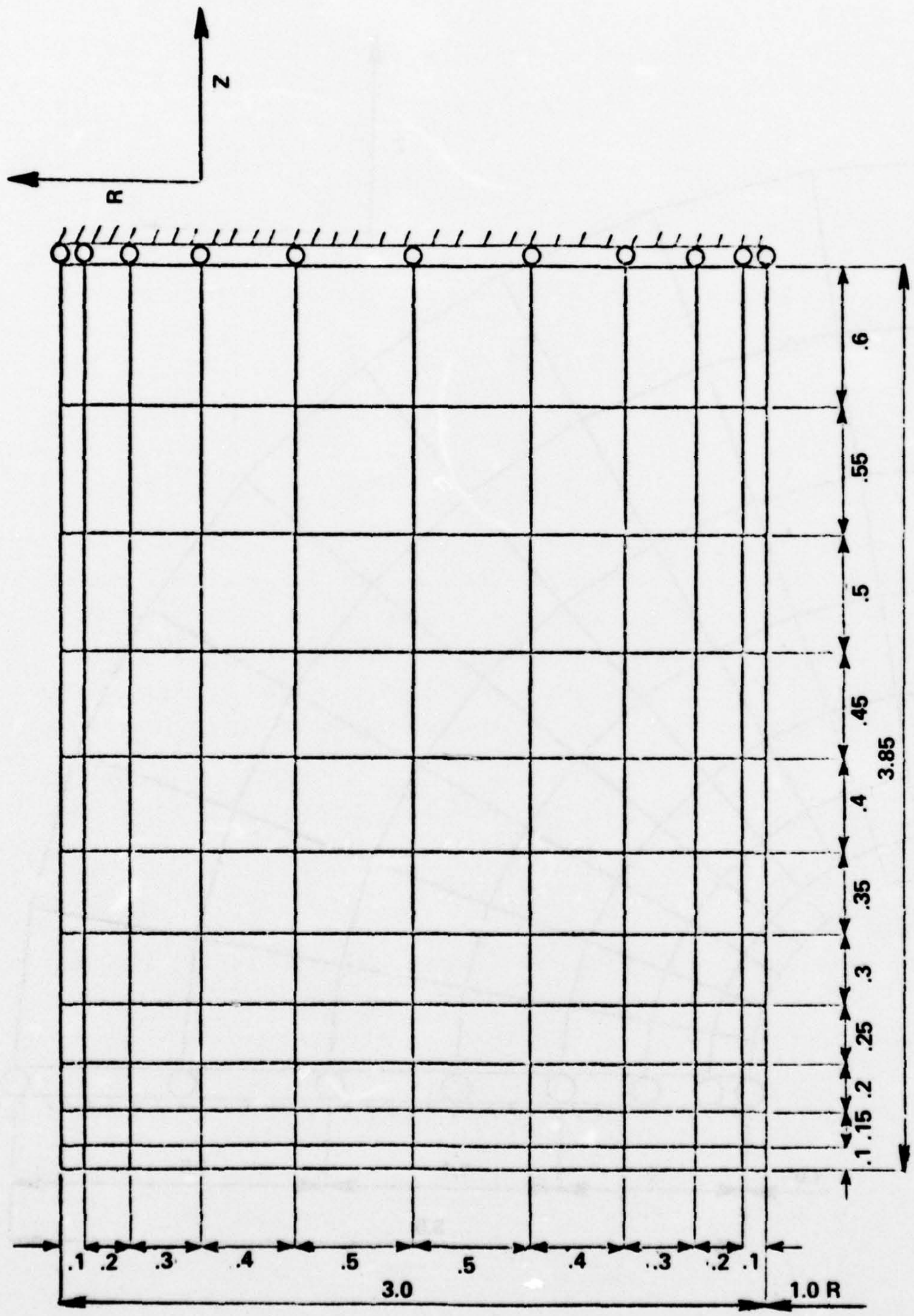

Figure 3. Grid for Problem Number 3

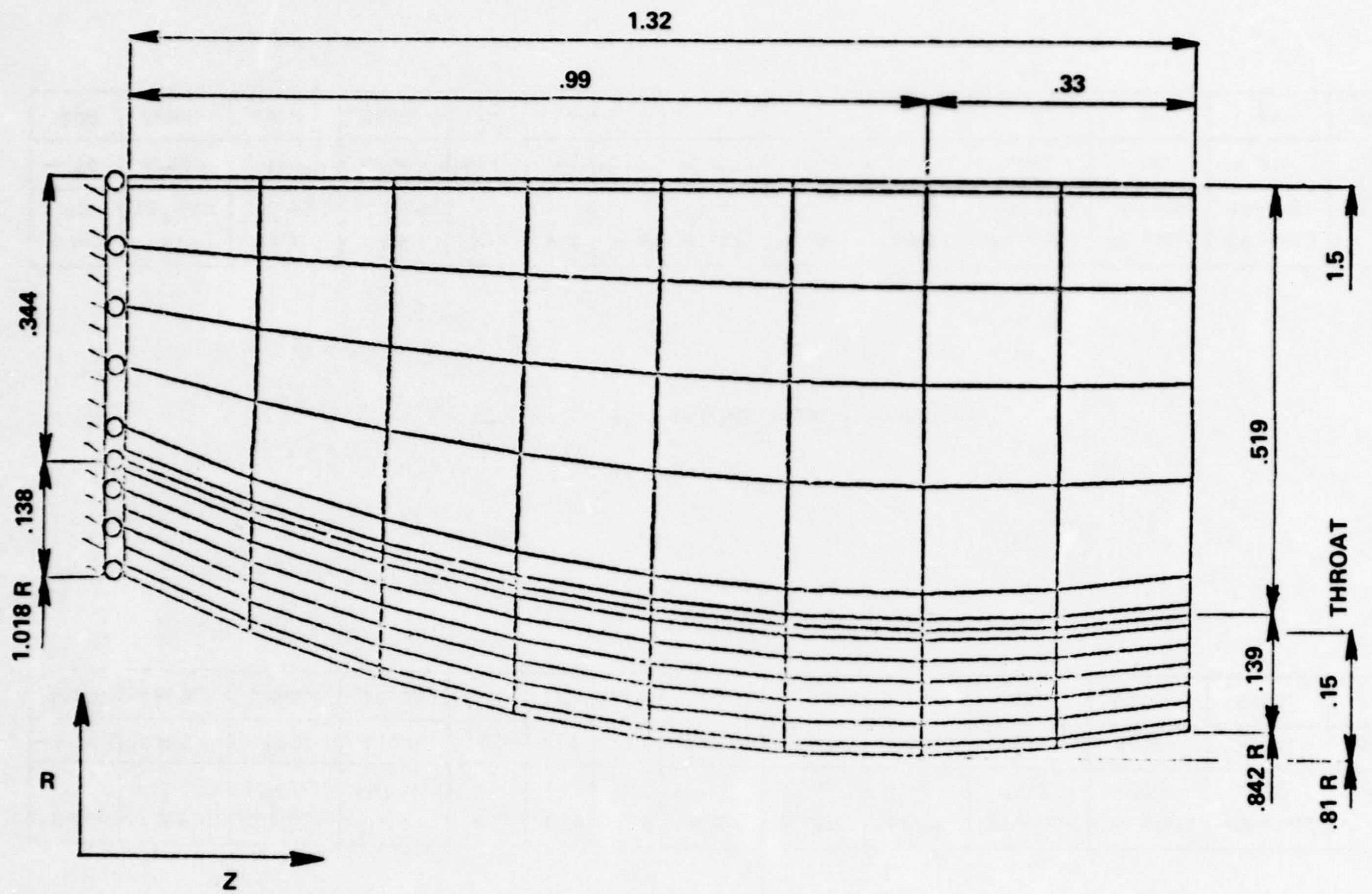

Figure 4. Grid for Problem Number 4

Table 1. ATJ Graphite Material Properties

Temp ^oF	Er 10^3 PSI	Ez 10^2 PSI	$E\theta$ 10^3 PSI	ν_{rz}	$\nu_{r\theta}$	$\nu_{z\theta}$	$\alpha_r\Delta T$ IN/IN	$\alpha_z\Delta T$ IN/IN	$\alpha_\theta\Delta T$ IN/IN	σ_r yield PSI	σ_z yield PSI	σ_θ yield PSI	G 10^3 PSI
70	1100.	800.	1100.	.138	.14	.10	-.0062	-.0076	-.0062	4500.	4100.	4500.	418.
3200	1650.	1060.	1650.	.28	.20	.18	-	-	-	5300.	4200.	5300.	530.

Table 2. SiC/PG Material Properties

Temp ^oF	Er 10^3 PSI	Ez 10^3 PSI	$E\theta$ 10^3 PSI	ν_{rz}	$\nu_{r\theta}$	$\nu_{z\theta}$	$\alpha_r\Delta T$ IN/IN	$\alpha_z\Delta T$ IN/IN	$\alpha_\theta\Delta T$ IN/IN	σ_r yield 10^3 PSI	σ_z yield 10^3 PSI	σ_θ yield 10^3 PSI	G 10^3 PSI
70	4700.	4700.	4700.	.14	.14	.14	-.0080	-.0071	-.0071	24.	24.	24.	2060.
3200	5800.	5800.	5800.	.14	.14	.14	-	-	-	24.	24.	24.	2540.

presents the exact numbers used in generating the plots and provides the material needed to perform more critical comparisons. Appendix A also contains tables of % error for selected cases (Tables A20-A27). These tables clearly define the amount of absolute and relative error for each of the codes.

In the following discussion all displacements will be nodal point displacements (midside displacements are included in TEXGAP results). On the other hand, the stresses and strains in all cases are given for the center of the element. Since the TEXGAP code is the only one which does not output stresses and strains at the element center and had to be calculated by hand by averaging the output values.

The locations of the stresses and strains output from TEXGAP depend upon the element type which was used. For the Quad element they are the midpoint of the four nodal points. For either element the center element values of stress and strain were calculated by summing the values at all four points and dividing by 4. This averaged value is the one which appears in the results.

The results for problems 1 and 2 include the exact solutions. The exact solutions were obtained from the classical equations for pressurized cylinders and spheres and are listed at the beginning of Appendix A.

The data for problem number 1 appear in Tables A1-A3 and plots 1-3 in Appendix A. As can be readily seen the agreement between all codes and the accuracy of each code are very good for this problem. It is especially good for radial displacement and strain. The TEXGAP Quad 8 element seems to provide an upper bound for all cases and, there is a tendency for SAAS III to be lower bound, at least in the circumferential direction. This is particularly apparent in plots 2 and 3.

The omission of data for NONSAP in the results for circumferential and radial strains is not an oversight. In its present form the NONSAP code does not output strains.

Tables A4-A8 and plots 4-8 of Appendix A contain the data for problem 2. It was at this point that problems with the axisymmetric solution in NONSAP were discovered. As a result NONSAP was not used for the remainder of the evaluation.

Again the agreement between codes and the accuracy of each code are very good. The tendency for TEXGAP Quad 8 and SAAS III to form respectively upper and lower data bounds is also present in this problem (see plots 5 and 7).

An unexpected result observed in this problem is the quite good results obtained with NEPSAP for displacements and strains using a Poisson's ratio of .4999. This element is not reformulated in the sense that the TEXGAP quad element is and yet the results obtained with it rivals the TEXGAP quad element for accuracy (see plots 4 and 6).

Based on the exact solutions for this problem, the stresses in a given direction should be the same for any value of Poisson's ratio. Only one code, TEXGAP, can be compared in this manner. Plot 8 shows that the results obtained from the TEXGAP quad element are very good for this case.

The results of problem number 3 are presented in plots 9-16 and Tables A9-A16. This problem is common for propellant grains, but in this case the small L/D should be noted.

For problem 3 the results for NEPSAP do not agree as well with the other codes for either value of Poisson's ratio. The difference becomes quite significant in some cases (e.g., circumferential strain, plots 12 and 13). There are two possible causes for the error observed, error in the thermal calculations or problems with the symmetry boundry condition. Since the results for problem 4, also a cool down problem, do not show the same amount of error and considering that amount of relative error increases with proximity to the plane of symmetry, the boundry condition is most probably the cause.

There are two schools of thought concerning strain output from the codes. One school of thought regards the dimensional change due to free thermal expansion as a thermal strain, and the output strain value includes this strain. The other school of thought considers the free thermal expansion to be separate from the strain, and therefore outputs purely mechanical strains. According to the first school of thought, a bar of material subjected to a temperature change while held between infinitely rigid walls and with no other loads acting undergoes a total strain of zero. According to the second school of thought, the strain in the bar is equal to the free thermal expansion which would occur without the restraint (but opposite in sign). Plot 13 shows that the NEPSAP and TEXGAP Quad elements include thermal strain in the output values.

For propellant grain problems, the stresses on a radial plane cutting the grain are perhaps more significant. A plane was passed through the grain at Z = 2.45 inches and values for all three stresses were compared (plots 14, 15, and 16). It should be noted again that a Poisson's ratio of .30 was used so that all codes could be compared. As can be seen, relative differences between the codes have increased, but the agreement for all stresses is still very good.

Results for the SIC/PG cool down problem are shown on plots 17, 18, and 19, and in Tables A17-A19. The plot of circumferential stress (plot 18) does not contain data for NEPSAP. This is due to the problem associated with the addition of the orthotropic material model in the axisymmetric solution. This was discussed previously in the section describing the installation of the codes.

The results from NEPSAP for this problem would be expected to show similar relative errors to those observed in the preceeding cool down problem. However, examination of plots 17, 18, and 19 do not show the amount of difference observed before. Indeed, the results for each of the codes agree very well. Two possible explanations exist to account for this discrepancy. The first is the magnitudes of the numbers. The matrix solution may be having trouble with the small numbers in the previous grain cool down problem. Secondly, this problem does not have a rigid boundary condition restraining the outside diameter.

Next to accuracy, run time, i.e. cost, is the most important parameter to the analyst. Table 3 shows execution times in seconds consumed by the central processor (CP time) for each of the codes in each problem. Also shown is the number of equations which had to be solved for each problem.

The fact which immediately stands out is the amount of time used by TEXGAP. However, the numbers shown in this table are not completely fair to the TEXGAP code. The table shows run times for the same number of elements that was used for the other codes. With the elements in the TEXGAP code, it is possible to use a much coarser mesh and still obtain results of similar accuracy obtained by the remaining codes using the grids shown. These elements would substantially reduce the run time for TEXGAP.

A second item which can be concluded from this table concerns NEPSAP. It is generally accepted that a general 3-D code is more expensive to run than the 2-D axisymmetric codes regardless of the problem being solved. This is caused

Table 3. Run Times for Codes

Plane Stress Cylinder		Run Time (C. P. sec)
Number of Equations = 144		
NEPSAP		15.86
NONSAP		5.82
TEXGAP	QUAD	140.38
	QUAD 8	71.90
SAAS III		11.05
Sphere		
Number of Equations = 144		
NEPSAP		14.51
TEXGAP	QUAD	139.58
	QUAD 8	71.75
SAAS III		11.82
Cylinder Under Shrinkage		
Number of Equations = 460		
NEPSAP		26.99
TEXGAP	QUAD	266.02
	QUAD 8	139.93
SAAS III		17.47
P. G. Cool Down		
Number of Equations = 525		
NEPSAP		30.33
TEXGAP	QUAD 8	159.08
SAAS III		21.43

by the use of sophisticated solution techniques and core requirements needed for higher order analyses (i.e. 3-D, nonlinear, etc.) to solve problems which do not require such sophistication. Although it is true that the run times shown are greater for NEPSAP than for SAAS III, the difference is not as great as might be expected. Considering also that NEPSAP required only 2000_8 locations more to load than SAAS III, the operating costs are very close.

USEABILITY OF CODES

The remarks on the useability of the codes is written from the point of view that one person is doing both the job of the analyst who writes up the data input in its proper format and the keypuncher who must punch the cards.

The simplest of the four codes from a user standpoint is, without question, TEXGAP. Its free-field input makes data input much easier than any of the other codes. The only restrictions which must be followed are the order of the data on each record (card) and to separate each item on the record with a comma. The mesh generation, element and boundary condition assignments are also much simpler than the other three codes and possibly simpler than any other code available to the analyst.

The biggest problem in using TEXGAP occurs when inputting material properties for orthotropic materials. TEXGAP requires manual input of the actual stiffness constants for this case instead of Young's Moduli and Poisson's ratios for the material directions.

SAAS III ranks second in useability. Its method for data input, which is typical for most codes, requires the user to use specific columns for the data. The mesh (if generated by the code) is specified by supplying line segments, straight or curved, which bound the region being modeled. The elements can only be generated internally in lines parallel to lines of constant I or J values. This requires several cards of input data to generate even the simplest geometries. Computation of the mesh in desired areas is possible, but the procedure is not simple to understand. It would require substantial work to become familiar with its use and probably some trial and error even then to get the desired mesh.

Several questions concerning some of the job control parameters came up when learning to use SAAS III. For example, it is not clear to the user that a 0 (zero) for the plane stress/plane strain option gives an axisymmetric solution.

Similarly for the stop parameter, it isn't obvious that a 0 (zero) makes the program do a complete solution. These things are minor but frustrating to the user. Much time digging through the program listing could be avoided by providing a complete set of options, including defaults, for all input parameter in the input guide. One final item which caused some question was the magnitudes of strain which the program outputs. After searching through the program listing, it was determined that the strains are output in percent; but neither the user manual nor the output states that fact. The user's guide is well written and is reasonably easy to understand. The only difficulties encountered in its use were associated with the loads data. There are several parameters on different data cards which control the loads data and the instructions lack a little detail concerning their use. Also it was discovered that two blank cards are needed at the end of the data to get a normal termination of the run.

NONSAP was used very little in this evaluation due to the problems encountered with the axisymmetric solution. Two items were discovered concerning the use of NONSAP. The first item is that any load, thermal or mechanical, must be converted to concentrated nodal loads externally. This considerably complicates the input of loads. The second item is the lack of strain output.

DEFICIENCIES OF CODES

In order to be able to describe the deficiencies of the current codes, the needed capabilities should first be defined. The features desired in a general purpose nozzle code were discussed in detail in Volume I of this report. To summarize the desired code, it would be a finite element code with 2-D axisymmetric and 3-D elements. It must be capable of analyzing a variety of materials that range from isotropic to fully anisotropic in character and allow temperature dependent properties. It must be capable of handling axisymmetric as well as non-axisymmetric loads. These loads would include concentrated pressure and thermal loads plus initial displacements and strains. The code must also allow material and kinematic (geometric) nonlinearities. And finally, it must be nonproprietary. These capabilities would form an adequate nozzle code.

There are several other capabilities deemed very desirable for this code, although they are not absolutely necessary. High on this list would be generation schemes for nodes and elements plus graphics, either on line or paper plots,

for developing the grids and displaying output. A system that allows multiple I - J grids and makes it possible to alter the grid of separate components without disturbing the entire model would be useful. Boundary conditions which allow adjacent components to slip or model gap closure would be very desirable. Also such things as compatible high and low order elements to allow maximum efficiency in gridding, in dynamic analysis capability, and in companion thermal analyses would be useful items.

Speaking in general terms, the chief deficiency for all codes appears to be the lack of a nonlinear anisotropic material model. The DOASIS code is the only one of the codes studied which has a theoretically sound nonlinear, small strain, anisotropic model. This model assumes the material has three mutually orthogonal principal axes, i.e. the material must be orthotropic. The small strain assumption is probably sufficient for most of the state of the art materials since most have a low strain to failure.

None of the codes currently used allow sliding contact or gap closure boundry conditions. These would be particularly useful for modeling throats made of PG washers, but there are numerous places in present nozzle designs which display these types of behavior.

Of the four codes which were run, NEPSAP* has the fewest deficiencies, but it still lacks some important capabilities. NEPSAP does not have an anisotropic axisymmetric element and also lacks a nonlinear anisotropic model.

As for NONSAP, the deficiencies are also in the lack of anisotropic material models. Most of the nonlinear capabilities in NONSAP are for isotropic materials and are useable for 2-D axisymmetric elements only. In addition, none of the material models allow temperature dependent properties. Finally, the code permits only concentrated model loads which, in the case of 2-D axisymmetric analysis, must be axisymmetric.

SAAS III is a 2-D axisymmetric code and therefore has no 3-D capabilities. The code's nonlinear capability consists solely of a bilinear curve fit on Young's modulus. This model must be used with much care given to determining its

*This refers to the version of NEPSAP obtained from ASIAC.

applicability. The level of anisotropy extends only to orthotropic materials and they must be axisymmetric. Finally, SAAS III does not allow non-axisymmetric loadings.

Like SAAS III, TEXGAP is a 2-D axisymmetric code and does not handle 3-D analysis, but it has no nonlinear capability at all. Again, like SAAS III, its level of anisotropy extends only to orthotropic materials and they must be axisymmetric. It allows concentrated loads only by approximation through a Fourier series expansion technique. Of most significance TEXGAP does not allow temperature dependent material properties nor analysis of a problem containing thermal gradients.

SECTION IV

CONCLUSIONS

The only surprising result uncovered in the program is the reasonably good values for displacements and strains obtained by NEPSAP with a Poisson's ratio near one-half. The accuracy of the results obtained by each of the four codes on all of the problems considered in this project is good. This is true for the relative agreement between the codes and for the absolute accuracy of each code in the problems with exact solutions.

None of the codes contained all nor most of the features desirable for a general purpose nozzle code, but many of these features were addressed by at least one of the codes if only for the isotropic, elastic case. This represents a basic understanding by the code developers for the needs of the analysts in the nozzle industry and provides a framework on which to build better codes.

The calculated strain values from any computer code must be viewed cautiously when solving problems involvong thermal expansion. The output values of strain may or may not contain the thermal strain depending on which code is being used. In one case using the TEXGAP code, these values even depended on which element was being used.

Based on the results of this program it is not necessarily true that the higher order elements give "better" results. While it is true that the higher order elements used in a coarser grid will provide comparable results with the standard elements, a blanket statement about better results can't be made. The determination of the point at which these elements begin to make visable payoffs when considering accuracy versus grid coarseness and run times deserves more investigation.

One final item, and one that is generally accepted as true but did not prove to be very significant, is the increased cost which must be paid to run a general 3-D code, over that of the standard 2-D axisymmetric codes, to analyze 2-D problems. If NEPSAP is accepted as a general 3-D code and the problems analyzed in this project considered as reasonably similar to typical problems, then the concept of user cost needs to be re-evaluated.

SECTION V

APPENDIX A

The results of the first two problems, internally pressurized cylinder and sphere respectively, were compared to results obtained from the classical solutions for these two problems. For convenience the equations used to determine the exact solutions are given below.*

Internally Pressurized Cylinder

$$\sigma_r = \frac{a^2 P_i}{b^2 - a^2}\left(1 - \frac{b^2}{r^2}\right)$$

$$\sigma_\theta = \frac{a^2 P_i}{b^2 - a^2}\left(1 + \frac{b^2}{r^2}\right)$$

$$\epsilon_r = \frac{1}{E}\left(\sigma_r - \nu\sigma_\theta\right)$$

$$\epsilon_\theta = \frac{1}{E}\left(\sigma_\theta - \nu\sigma_r\right)$$

$$U_r = r\epsilon_\theta$$

*Theory of Elasticity, Third Edition, Timoshenko and Goodier, pp. 70-71 and pp. 392-395.

Internally Pressurized Sphere

$$\sigma_r = \frac{P_i a^3}{r^3} \frac{(b^3 - r^3)}{(a^3 - b^3)}$$

$$\sigma_\theta = \frac{P_i a^3}{2r^3} \frac{(2r^3 + b^3)}{(b^3 - a^3)}$$

$$\epsilon_r = \frac{1}{E} \left|\sigma_r - \nu(2\sigma_\theta)\right| \quad \sigma_z = \sigma_\theta$$

$$\epsilon_\theta = \frac{1}{E} \left|\sigma_\theta - \nu(\sigma_r + \sigma_\theta)\right|$$

$$U = r\epsilon_\theta$$

Table A-1

Plane Stress Cylinder (Nu = .4999)
Radial Displacement (inches) Vs Radial Position (inches)

Radial Position	Exact Solution	NEPSAP	NONSAP 4 Node Elem.	NONSAP 8 Node Elem.	TEXGAP Quad 8 Elem.	TEXGAP Quad Elem.	SAAS III
1.0	.16038	.1589	.15844	.16396	.15958	.15952	.15766
1.1	.14630			.14761	.14556	.14556	
1.2	.13460	.1332	.13293	.13366	.13392	.13392	.13227
1.35	.12038			.12217	.11977	.11978	
1.5	.10908	.1079	.10775	.10931	.10854	.10854	.10721
1.7	.09723			.09731	.09675	.09675	
1.9	.08798	.08694	.08695	.08792	.08755	.08755	.08652
2.15	.07897			.07895	.07859	.07859	
2.4	.07198	.07110	.07119	.07199	.07164	.07164	.07084
2.7	.06545			.06546	.06515	.06515	
3.0	.06039	.05965	.05979	.06038	.06012	.06012	.05949
3.35	.05580			.05580	.05556	.05556	
3.7	.05226	.05164	.05179	.05226	.05204	.05204	.05153
4.1	.04913			.04914	.04893	.04894	
4.5	.04675	.04622	.04638	.04675	.04657	.04659	.04615

Table A-2

Plane Stress Cylinder (Nu = .4999)
Circumferential Stress (P.S.I.) Vs Radial Position (inches)

Radial Position	Exact Solution	NEPSAP	NONSAP 4 Node Elem.	NONSAP 8 Node Elem.	TEXGAP Quad 8 Elem.	TEXGAP Quad Elem.	SAAS III
1.1	92.13	90.24	91.21	91.88	95.29	91.42	87.
1.35	62.91	61.84	62.97	63.72	66.26	62.95	59.
1.7	41.59	40.91	41.81	41.39	43.99	41.73	39.
2.15	27.95	27.50	28.09	27.79	29.41	28.03	26.
2.7	19.62	19.32	19.68	19.51	20.46	19.64	19.
3.35	14.57	14.39	14.58	14.48	15.04	14.55	14.
4.1	11.45	11.36	11.44	11.39	11.72	11.42	11.

Table A-3

Plane Stress Cylinder (Nu = .4999)
Circumferential Strain (in./in.) Vs Radial Position (inches)

Radial Position	Exact Solution	NEPSAP	TEXGAP Quad 8 Elem.	TEXGAP Quad Elem.	SAAS III
1.1	.13300	.1307	.1336	.1316	.1277
1.35	.08917	.08798	.09066	.08894	.08531
1.7	.05719	.05644	.05838	.05720	.05468
2.15	.03673	.03620	.03744	.03672	.03518
2.7	.02424	.02386	.02461	.02418	.02329
3.35	.01666	.01641	.01684	.01658	.01606
4.1	.01198	.01184	.01206	.01191	.01160

Table A-4

Sphere Under Internal Pressure (Nu = .4999)
Radial Stress (P. S. I.) Vs Radial Position (inches)

Radial Position	Exact Solution	TEXGAP Quad Elem.
1.1	-74.86	-74.93
1.35	-39.99	-40.49
1.7	-19.47	-19.79
2.15	-9.06	-9.27
2.7	-4.03	-4.09
3.35	-1.58	-1.60
4.1	-.3575	-.3795

Table A-5

Sphere Under Internal Pressure (Nu = .30)
Circumferential Stress (P.S.I.) Vs Radial Position (inches)

Radial Position	Exact Solution	NEPSAP	TEXGAP Quad 8 Elem.	TEXGAP Quad Elem.	SAAS III
1.1	39.09	37.88	42.38	38.95	38.
1.35	21.66	21.06	24.51	21.95	22.
1.7	11.40	11.07	13.02	11.62	11.
2.15	6.20	6.02	6.98	6.30	6.
2.7	3.68	3.58	4.03	3.72	4.
3.35	2.45	2.40	2.62	2.47	2.
4.1	1.84	1.82	1.92	1.85	2.

Table A-6

Sphere Under Internal Pressure (Nu = .4999)
Circumferential Strain (in. /in.) Vs Radial Position (inches)

Radial Position	Exact Solution	NEPSAP	TEXGAP Quad. Elem.
1.1	.05697	.05607	.05626
1.35	.03082	.03054	.03088
1.7	.01543	.01528	.01554
2.15	.007630	.007527	.007672
2.7	.003853	.003774	.003859
3.35	.002017	.001961	.002011
4.1	.001100	.001067	.001092

Table A-7

Sphere Under Internal Pressure (Nu = .30)
Circumferential Strain (in./in.) Vs Radial Position (inches)

Radial Position	Exact Solution	NEPSAP	TEXGAP Quad 8 Elem.	TEXGAP Quad Elem.	SAAS III
1.1	.04982	.04904	.05077	.04938	.04968
1.35	.02716	.02695	.02834	.02734	.02738
1.7	.01382	.01372	.01454	.01399	.01400
2.15	.007057	.006974	.007400	.007133	.00715
2.7	.003783	.003719	.003932	.003807	.00382
3.35	.002192	.002150	.002254	.002181	.00221
4.1	.001397	.001374	.001423	.001394	.00140

Table A-8

Sphere Under Internal Pressure
Radial Stress (P.S.I.) Vs Radial Position (inches)

Radial Position	Exact Solution	Nu = .4999 TEXGAP Quad. Elem.	Nu = .30 TEXGAP Quad. Elem.
1.1	-74.86	-74.93	-75.11
1.35	-39.99	-40.49	-40.63
1.7	-19.47	-19.79	-19.88
2.15	-9.06	-9.21	-9.26
2.7	-4.03	-4.09	-4.11
3.35	-1.58	-1.60	-1.61
4.1	-.3575	-.3795	-.3829

Table A-9

Cylinder Under Shrinkage (Nu = .4999)
Radial Displacement (inches) Vs Axial Position (inches)

Axial Position	NEPSAP	TEXGAP Quad. Elem.	Thiokol Isopara. Elem.
0.	.01499	.01124	.01350
.05		.01265	
.1	.01758	.01406	.01417
.175		.01618	
.25	.02158	.01832	.01843
.35		.02117	
.45	.02704	.02403	.02414
.575		.02756	
.7	.03368	.03102	.03113
.85		.03504	
1.0	.04103	.03886	.03897
1.175		.04301	
1.35	.04838	.04681	.04697
1.55		.05082	
1.75	.05506	.05430	.05440
1.975		.05769	
2.2	.06063	.06056	.06064
2.45		.06316	
2.7	.06475	.06525	.06532
2.975		.06696	
3.25	.06727	.06819	.06826
3.55		.06895	
3.85	.06810	.06923	.06930

Table A-10

Cylinder Under Shrinkage (Nu = .30)
Radial Displacement (inches) Vs Axial Position (inches)

Axial Position	NEPSAP	TEXGAP Quad 8 Elem.	TEXGAP Quad Elem.	SAAS III
0.	.008267	.007833	.007826	.007758
.05		.008318	.008310	
.1	.009137	.008804	.008795	.008709
.175		.009535	.009527	
.25	.01052	.01027	.01026	.01018
.35		.01125	.01124	
.45	.01242	.01222	.01221	.01214
.575		.01341	.01340	
.7	.01474	.01456	.01455	.01450
.85		.01586	.01585	
1.0	.01728	.01707	.01707	.01705
1.175		.01836	.01835	
1.35	.01977	.01950	.01949	.01951
1.55		.02063	.02062	
1.75	.02192	.02158	.02158	.02161
1.975		.02246	.02245	
2.2	.02356	.02315	.02315	.02318
2.45		.02375	.02375	
2.7	.02465	.02419	.02419	.02422
2.975		.02453	.02453	
3.25	.02523	.02476	.02476	.02478
3.55		.02490	.02490	
3.85	.02538	.02495	.02495	.02496

Table A-11

Cylinder Under Shrinkage (Nu = .30)
Axial Stress (P.S.I.) Vs Axial Position (inches)

Axial Position	NEPSAP	TEXGAP Quad 8 Elem.	TEXGAP Quad Elem.	SAAS III
.05	.1053	.01725	-.003722	0.
.175	.04192	-.04473	-.08224	-0.
.35	-.1968	-.2520	-.2816	-0.
.575	-.5178	-.5058	-.5250	-1.
.85	-.7151	-.5920	-.6038	-1.
1.175	-.5411	-.2606	-.2723	-0.
1.55	.1775	.6360	.6156	1.
1.975	1.394	2.04	2.00	2.
2.45	2.87	3.67	3.61	4.
2.975	4.17	5.13	5.06	5.
3.55	5.21	6.02	5.94	6.

Table A-12

Cylinder Under Shrinkage (Nu = .4999)
Circumferential Strain (in./in.) Vs Axial Position (inches)

Axial Position	NEPSAP	TEXGAP Quad. Elem.	Thiokol Isopara. Elem.
.05	.01432	.01112	.01144
.175	.01731	.01443	.01470
.35	.02143	.01910	.01935
.575	.02694	.02508	.02532
.85	.03284	.03205	.03230
1.175	.03923	.03948	.03974
1.55	.04460	.04652	.04694
1.975	.04923	.05299	.05327
2.45	.05207	.05799	.05826
2.975	.05374	.06145	.06169
3.55	.05338	.06324	.06346

Table A-13

Cylinder Under Shrinkage (Nu = .30)
Circumferential Strain (in. /in.) Vs Axial Position (inches)

Axial Position	NEPSAP	TEXGAP Quad 8 Elem.	TEXGAP Quad Elem.	SAAS III	NEPSAP Thermal Strain Removed	TEXGAP Quad Elem. Thermal Strain Removed
.05	.007509	.01729	.007241	.01715	.01751	.01724
.175	.008501	.01844	.008388	.01830	.01850	.01839
.35	.009940	.02005	.01000	.01991	.01994	.02000
.575	.01177	.02208	.01203	.02196	.02177	.02203
.85	.01385	.02437	.01433	.02427	.02385	.02433
1.175	.01592	.02670	.01667	.02662	.02592	.02667
1.55	.01771	.02881	.01878	.02874	.02771	.02878
1.975	.01902	.03051	.02048	.03045	.02902	.03048
2.45	.01971	.03171	.02168	.03165	.02971	.03168
2.975	.01994	.03245	.02240	.03237	.02994	.03240
3.55	.01957	.03279	.02274	.03270	.02957	.03274

Table A-14

Cylinder Under Shrinkage (Nu = .30)
Radial Stress (P.S.I.) at Z = 2.45 in. Vs Radial Position (inches)

Radial Position	NEPSAP	TEXGAP Quad 8 Elem.	TEXGAP Quad Elem.	SAAS III
1.05	1.06	1.63	1.55	2.
1.2	4.68	5.34	5.15	5.
1.45	8.50	9.12	8.91	9.
1.8	11.40	11.91	11.74	12.
2.25	13.12	13.56	13.42	13.
2.75	13.78	14.13	14.04	14.
3.2	13.75	14.00	13.95	14.
3.55	13.48	13.66	13.64	14.
3.8	13.22	13.37	13.36	13.
3.95	13.06	13.20	13.17	13.

Table A-15

Cylinder Under Shrinkage (Nu = .30)
Axial Stress (P.S.I.) at Z = 2.45 in. Vs Radial Position (inches)

Radial Position	NEPSAP	TEXGAP Quad 8 Elem.	TEXGAP Quad Elem.	SAAS III
1.05	2.87	3.67	3.61	4.
1.2	3.52	4.19	4.06	4.
1.45	4.58	5.03	4.88	5.
1.8	6.10	6.37	6.23	6.
2.25	8.32	8.49	8.35	8.
2.75	11.25	11.34	11.23	11.
3.2	14.25	14.29	14.24	14.
3.55	16.72	16.76	16.74	17.
3.8	18.48	18.53	18.53	19.
3.95	19.51	19.58	19.57	20.

Table A-16

Cylinder Under Shrinkage (Nu = .30)
Circumferential Stress (P.S.I.) at Z = 2.45 in. Vs Radial Position (inches)

Radial Position	NEPSAP	TEXGAP Quad 8 Elem.	TEXGAP Quad Elem.	SAAS III
1.05	30.89	33.30	33.23	33.
1.2	28.07	29.95	29.72	30.
1.45	25.09	26.35	26.10	26.
1.8	22.81	23.58	23.38	23.
2.25	21.35	21.83	21.69	22.
2.75	20.58	20.87	20.79	21.
3.2	20.22	20.40	20.36	20.
3.55	20.03	20.16	20.15	20.
3.8	19.91	20.02	20.02	20.
3.95	19.84	19.94	19.94	20.

Table A-17

SiC/PG Cooldown (Throat plane)
Radial Displacement (inches) Vs Radial Position (inches)

Radial Position	NEPSAP	TEXGAP Quad 8 Elem.	SAAS III
.810	-.005401	-.005395	-.005400
.8165		-.005447	
.823	-.005506	-.005499	-.005501
.8355		-.005600	
.848	-.005707	-.005700	-.005701
.8605		-.005800	
.873	-.005907	-.005900	-.005901
.8855		-.006000	
.898	-.006107	-.006100	-.006101
.9105		-.006199	
.923	-.006307	-.006299	-.006301
.9355		-.006399	
.948	-.006506	-.006498	-.006500
.954		-.006548	
.960	-.006602	-.006598	-.006600
.9665		-.006635	
.973	-.006678	-.006672	-.006673
.9885		-.006764	
1.004	-.006862	-.006856	-.006857
1.068		-.007218	
1.132	-.007629	-.007581	-.007629
1.193		-.007947	
1.254	-.008369	-.008314	-.008367
1.313		-.008683	
1.372	-.009089	-.009053	-.009086
1.430		-.009424	
1.488	-.009801	-.009796	-.009798
1.494		-.009833	
1.500	-.009875	-.009870	-.009875

Table A-18

SiC/PG Cooldown (Throat plane)
Circumferential Stress (P.S.I.) Vs Radial Position (inches)

Radial Position	TEXGAP Quad 8 Elem.	SAAS III
.8165	1920.	1955.
.8355	1774.	1804.
.8605	1589.	1612.
.8855	1416.	1432.
.9105	1252.	1263.
.9355	1096.	1108.
.954	983.	990.
.9665	-680.	-679.
.9885	-658.	-660.
1.068	-599.	-598.
1.193	-523.	-521.
1.313	-467.	-467.
1.430	-425.	-426.
1.494	-404.	-407.

Table A-19

SiC/PG Cooldown (Throat Plane)
Circumferential Strain (in./in.) Vs Radial Position (inches)

Radial Position	NEPSAP Thermal Strain Removed	TEXGAP Quad. 8 Elem.	SAAS III
.8165	.000420	.0004308	.00042
.8355	.000383	.0004001	.00039
.8605	.000345	.0003614	.00035
.8855	.000309	.0003256	.00032
.9105	.000277	.0002923	.00029
.9355	.000246	.0002609	.00025
.954	.000227	.0002384	.00023
.9665	-.000669	-.0006628	-.00067
.9885	-.000645	-.0006432	-.00065
1.068	-.000580	-.0005844	-.00058
1.193	-.000502	-.0005063	-.00050
1.313	-.000446	-.0004480	-.00045
1.430	-.000403	-.0004034	-.00040
1.494	-.000385	-.0003823	-.00039

Table A-20

Error (%) Based on Exact Solution
Plane Stress Cylinder - Radial Displacement

Radial Location	NONSAP 4 Node Elem.	NONSAP 8 Node Elem.	TEXGAP Quad 8 Elem.	TEXGAP Quad Elem.	SAAS III	NEPSAP
1.0	-1.2	2.2	-.5	-.5	-1.7	- .9
1.9	-1.2	-.1	-.4	-.4	-1.7	-1.2
4.5	-.8	0.	-.4	-.4	-1.3	-1.1

Table A-21

Error (%) Based on Exact Solution
Plane Stress Cylinder - Radial Stress

Radial Location	NEPSAP	NONSAP 4 Node Elem.	NONSAP 8 Node Elem.	TEXGAP Quad 8 Elem.	TEXGAP Quad Elem.	SAAS III
1.1	-.8	-2.2	-.3	-6.2	-1.7	-.9
2.15	-.9	-3.5	-.9	-8.5	-1.0	2.5
4.1	-10.3*	-15.7*	-6.3*	-35.5*	-8.3*	-5.9*

*Values of stress are very small at this location.

Table A-22

Error (%) Based on Exact Solution
Sphere (Nu = .30) Radial Displacement

Radial Location	NEPSAP	TEXGAP Quad 8 Elem.	TEXGAP Quad Elem.	SAAS III
1.0	-.3	-.8	-.8	-2.7
1.9	.2	-.8	-.8	-2.6
4.5	2.6	-.5	-.4	-1.5

Table A-23

Error (%) Based on Exact Solution
Sphere (Nu = .30) - Circumferential Stress

Radial Location	NEPSAP	TEXGAP Quad 8 Elem.	TEXGAP Quad Elem.	SAAS III
1.0	-3.1	8.4	-.4	-2.8
2.15	-2.9	12.6	1.6	-3.2
4.1	-1.3	4.1	.1	8.5

Table A-24

Relative Error (%) Based on TEXGAP Quad Element*
Cylinder Under Shrinkage (Nu = . 30) - Radial Displacement

Axial Location	NEPSAP	TEXGAP Quad 8 Elem.	SAAS III
0.	5.6	.1	-.8
.7	1.3	.1	-.3
2.2	1.8	0.	.2
3.85	1.7	0.	0.

*The TEXGAP Quad Element was chosen as the norm since it consistently had the smallest error in the first two problems.

Table A-25

Relative Error (%) Based on TEXGAP Quad Element
Cylinder Under Shrinkage (Nu = .30) - Circumferential Stress

Radial Location	NEPSAP	TEXGAP Quad 8 Elem.	SAAS III
1.05	-7.0	.2	-.7
2.25	-1.6	.7	1.4
3.95	-.5	0.	.3

Table A-26

Relative Error (%) Based on SAAS III*
SiC/PG Cooldown (Throat plane) - Radial Displacement

Radial Location	NEPSAP	TEXGAP Quad 8 Elem.
.810	0.	-.1
.848	.1	0.
.923	.1	0.
.960	0.	0.
1.004	0.	0.
1.372	0.	-.4
1.500	0.	0.

*The TEXGAP Quad element could not be used for this problem due to the lack of an Orthotropic material model. Therefore, SAAS III was chosen as the basis.

Table A-27

Relative Error (%) Based on SAAS III
SiC/PG Cooldown (Throat plane) - Circumferential Strain

Radial Location	NEPSAP	TEXGAP Quad 8 Elem.
.8165	0.	2.6
.8605	-1.4	3.6
.9105	-4.5	.8
.954	-1.3	3.7
.9665	-.1	-1.1
1.068	0.	.8
1.313	-.9	-.4
1.494	-1.3	-2.0

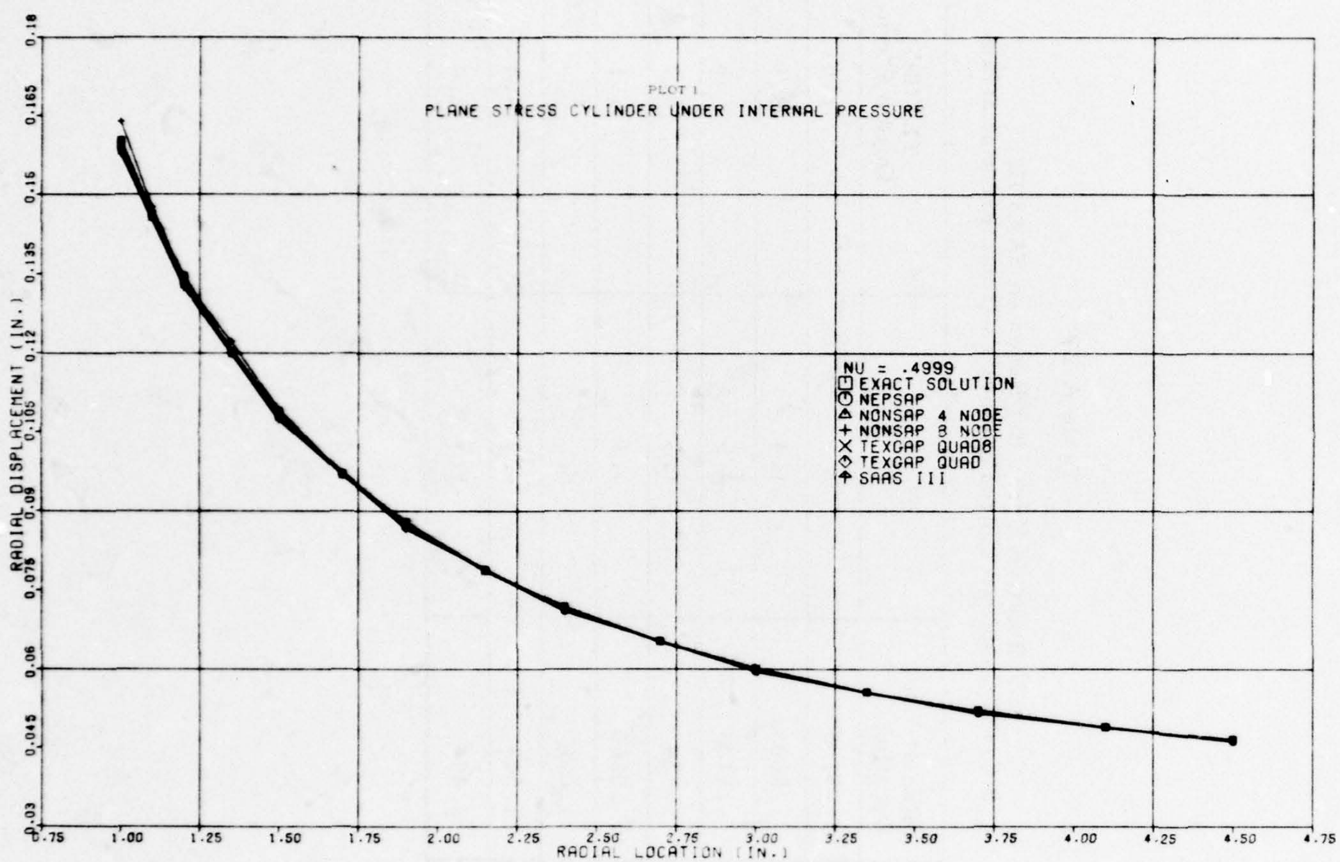

Figure A-1. Radial Displacement Vs Radial Location

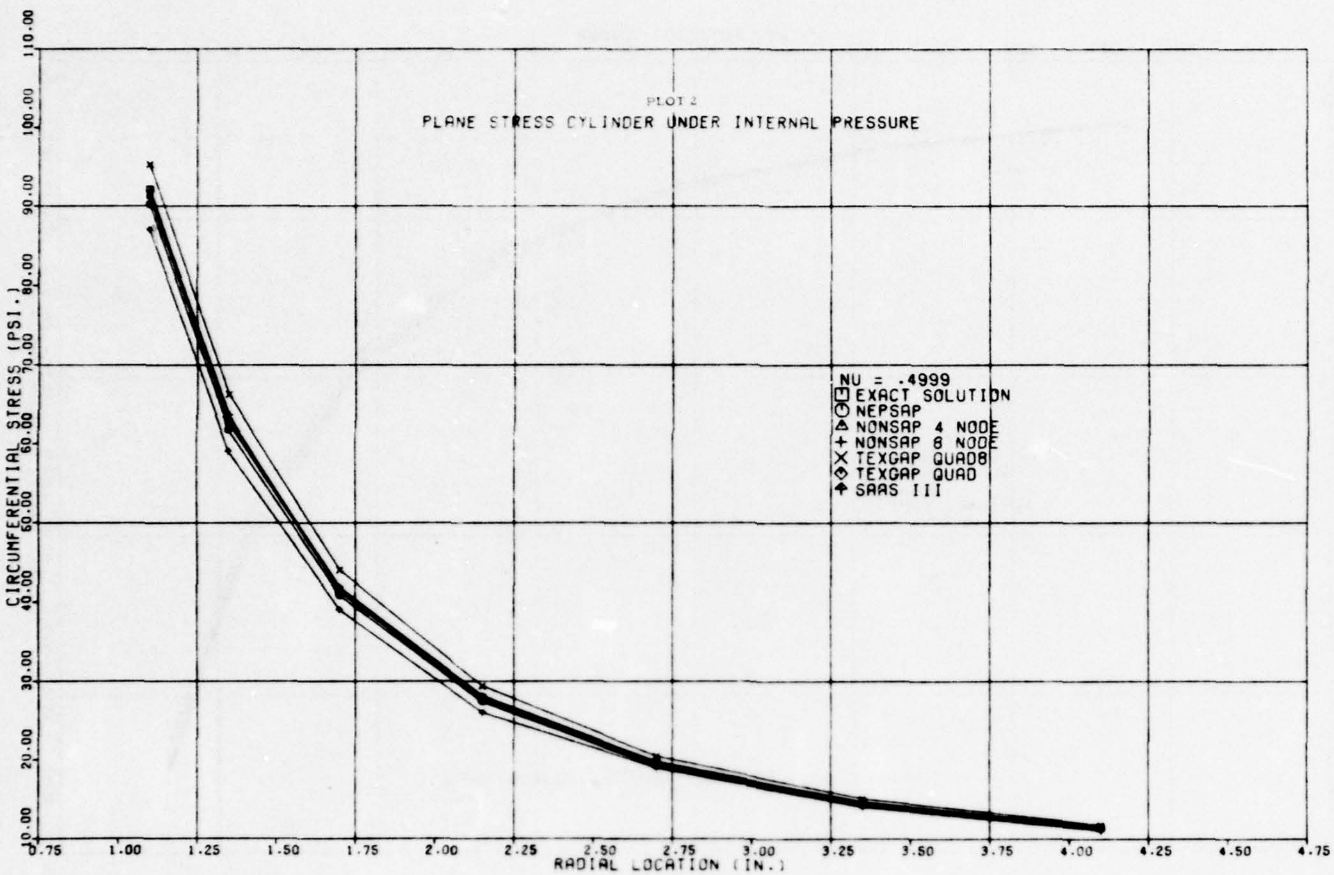

Figure A-2. Circumferential Stress Vs Radial Location

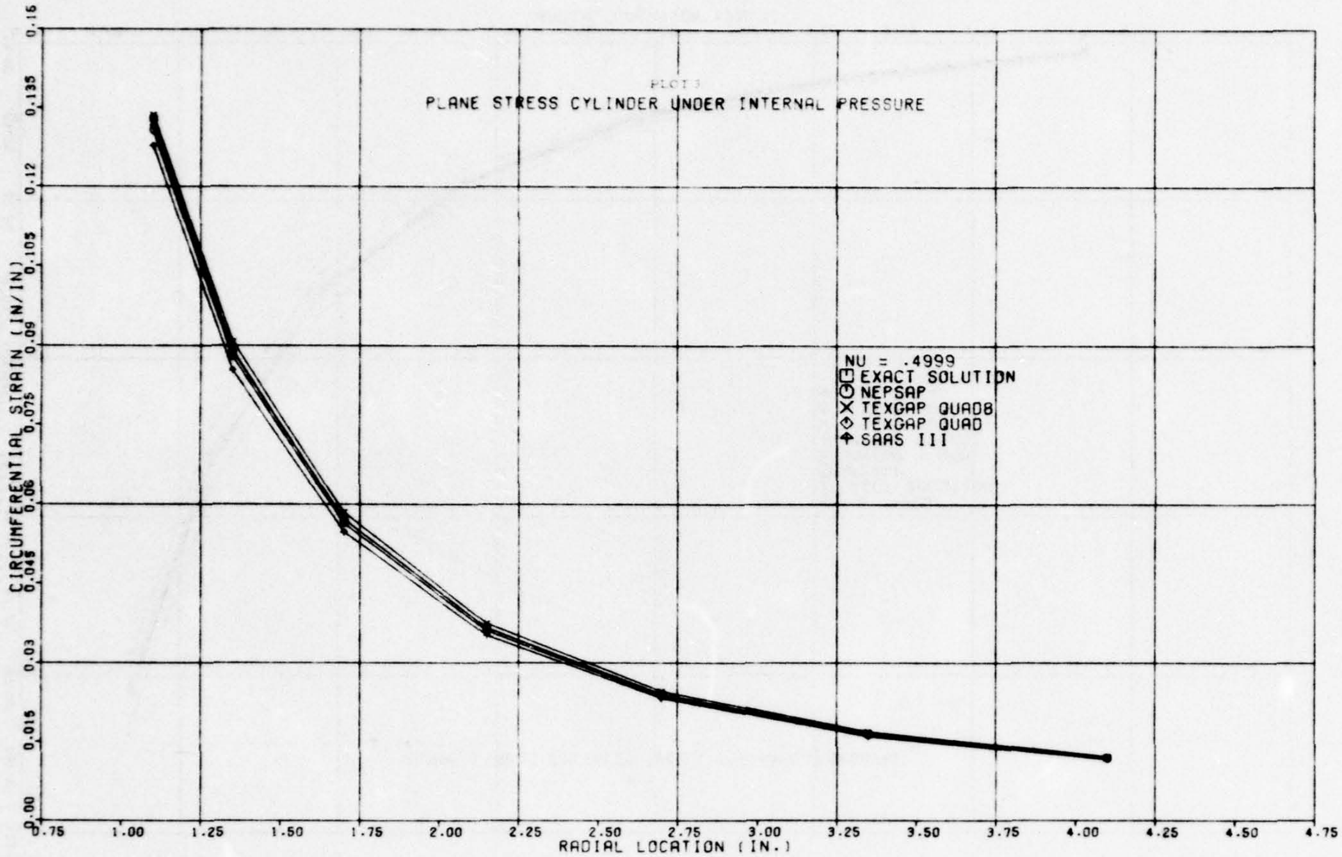

Figure A-3. Circumferential Strain Vs Radial Location

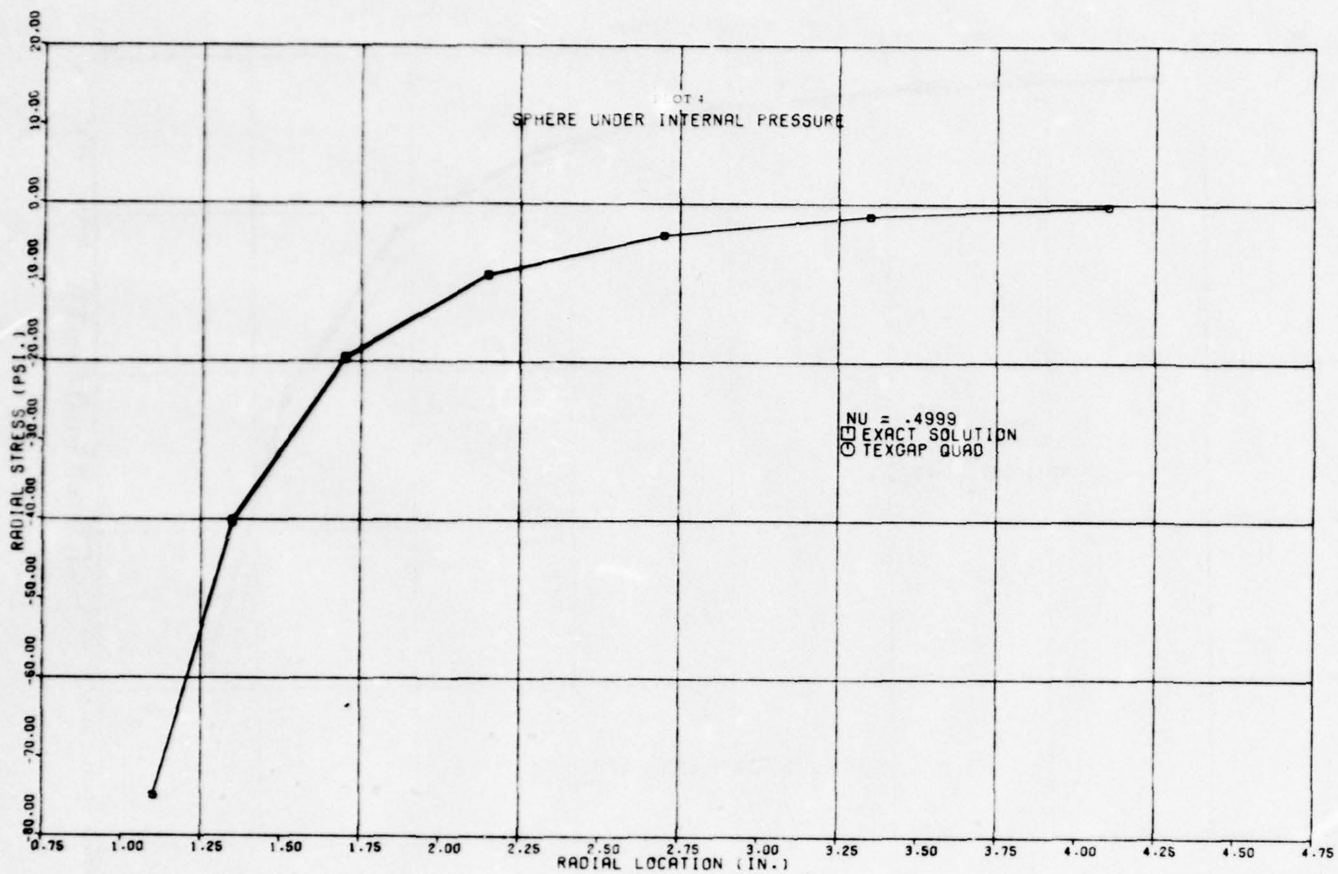

Figure A-4. Radial Stress Vs Radial Location

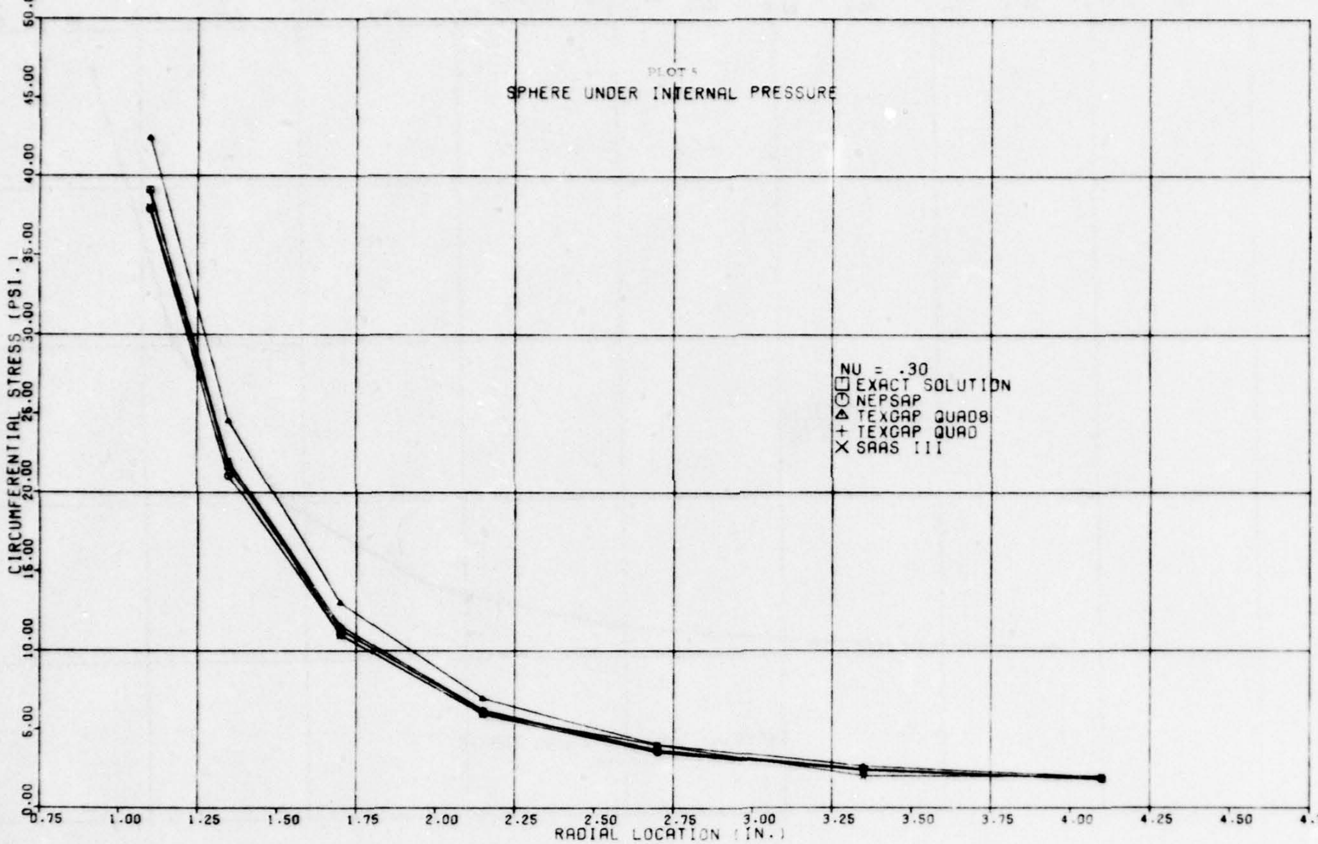

Figure A-5. Circumferential Stress Vs Radial Location

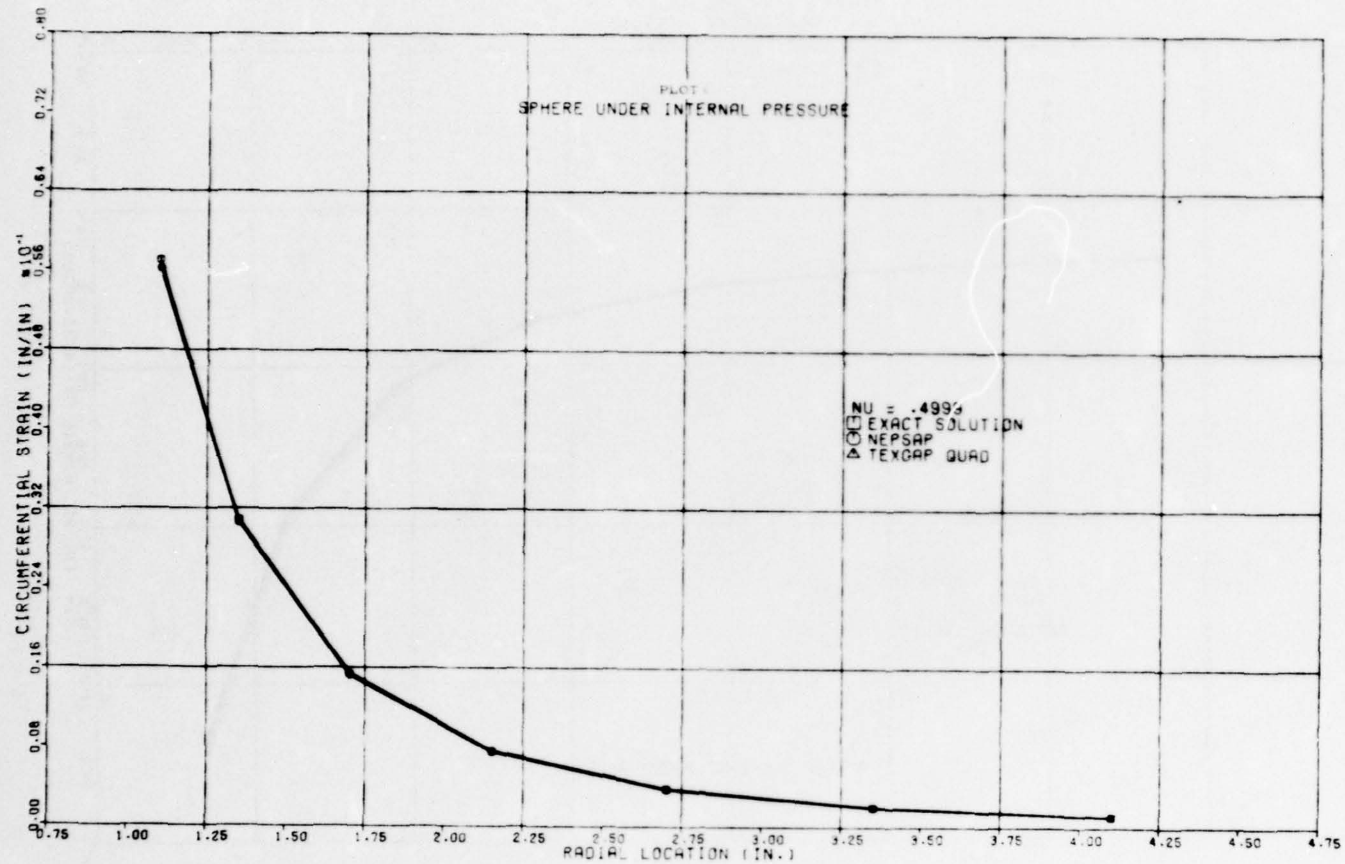

Figure A-6. Circumferential Strain Vs Radial Location

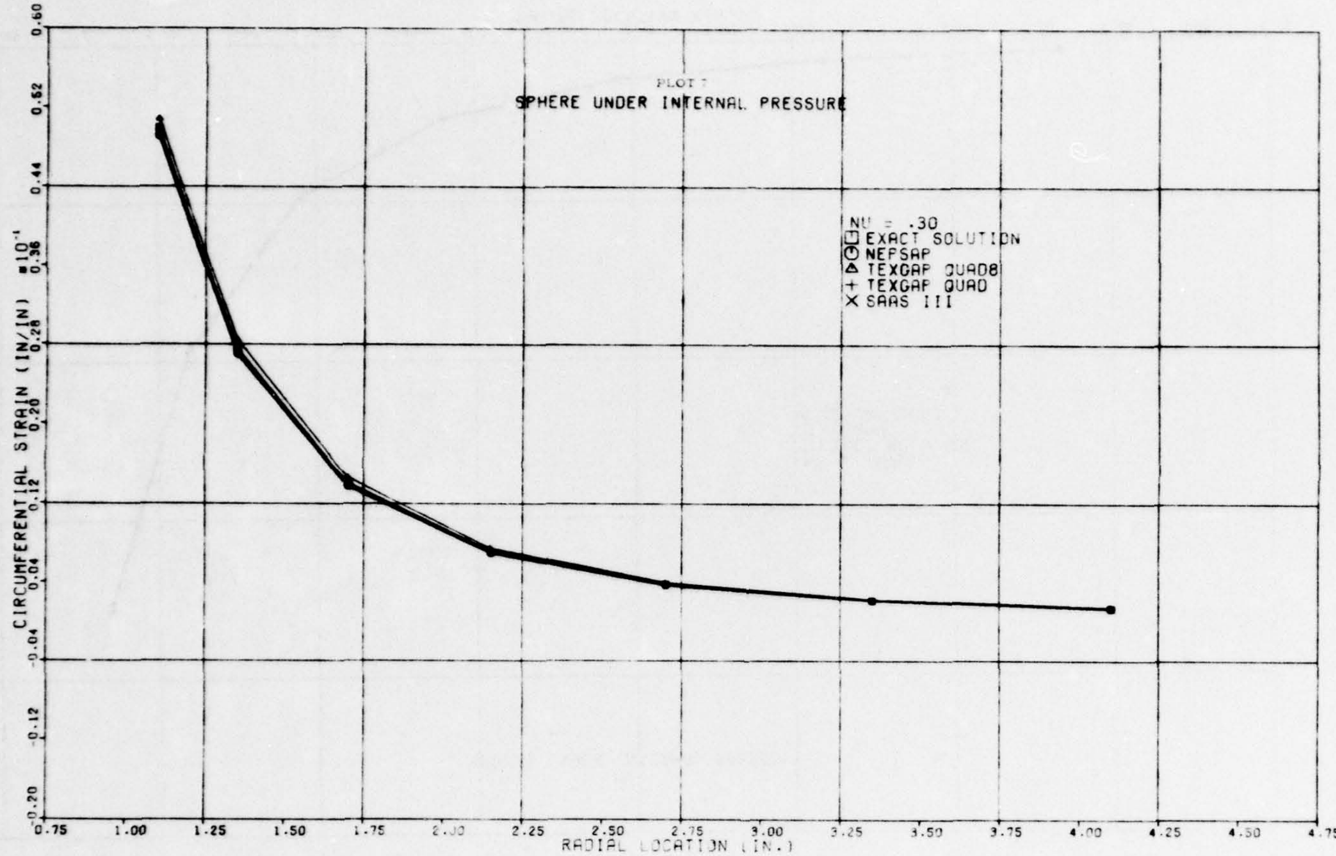

Figure A-7. Circumferential Strain Vs Radial Location

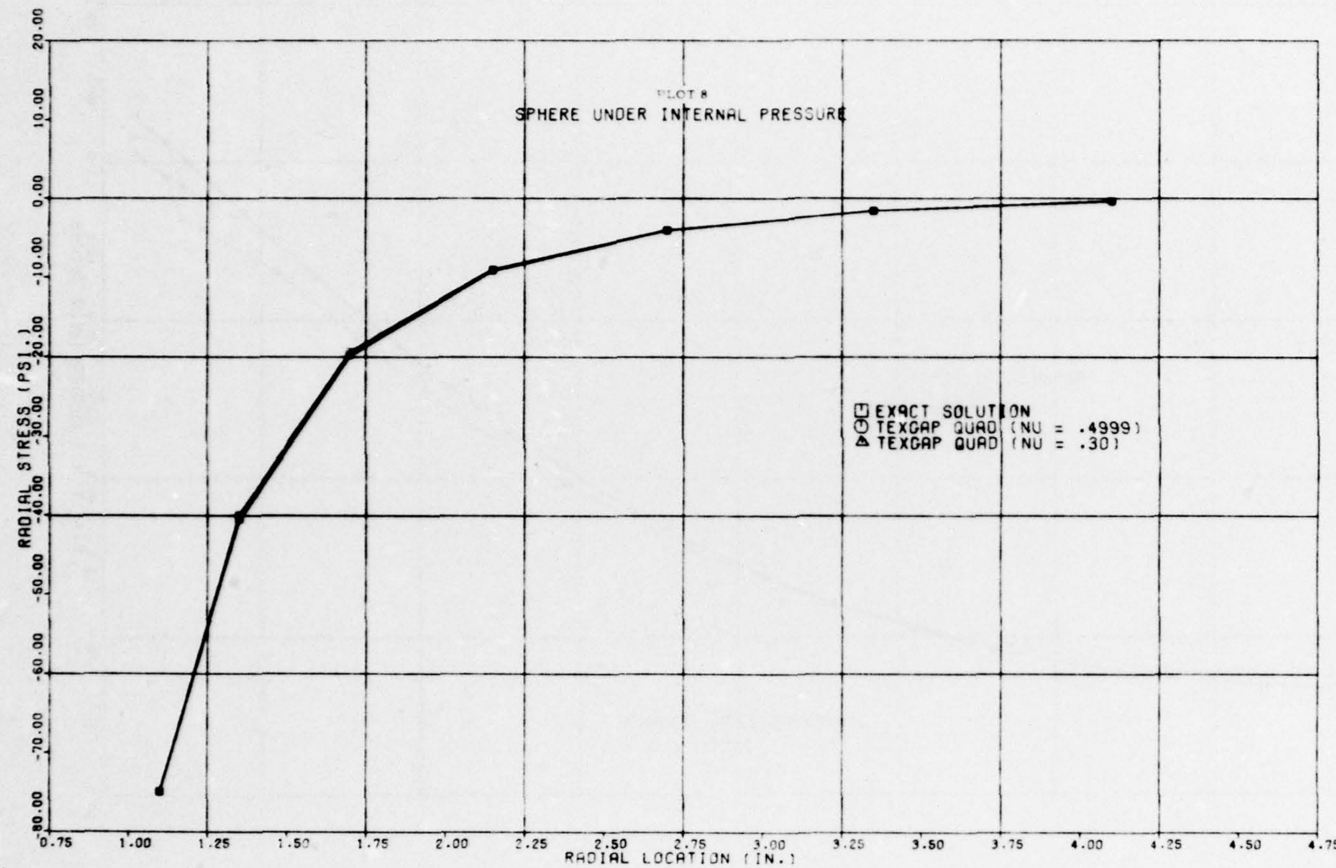

Figure A-8. Radial Stress Vs Radial Location

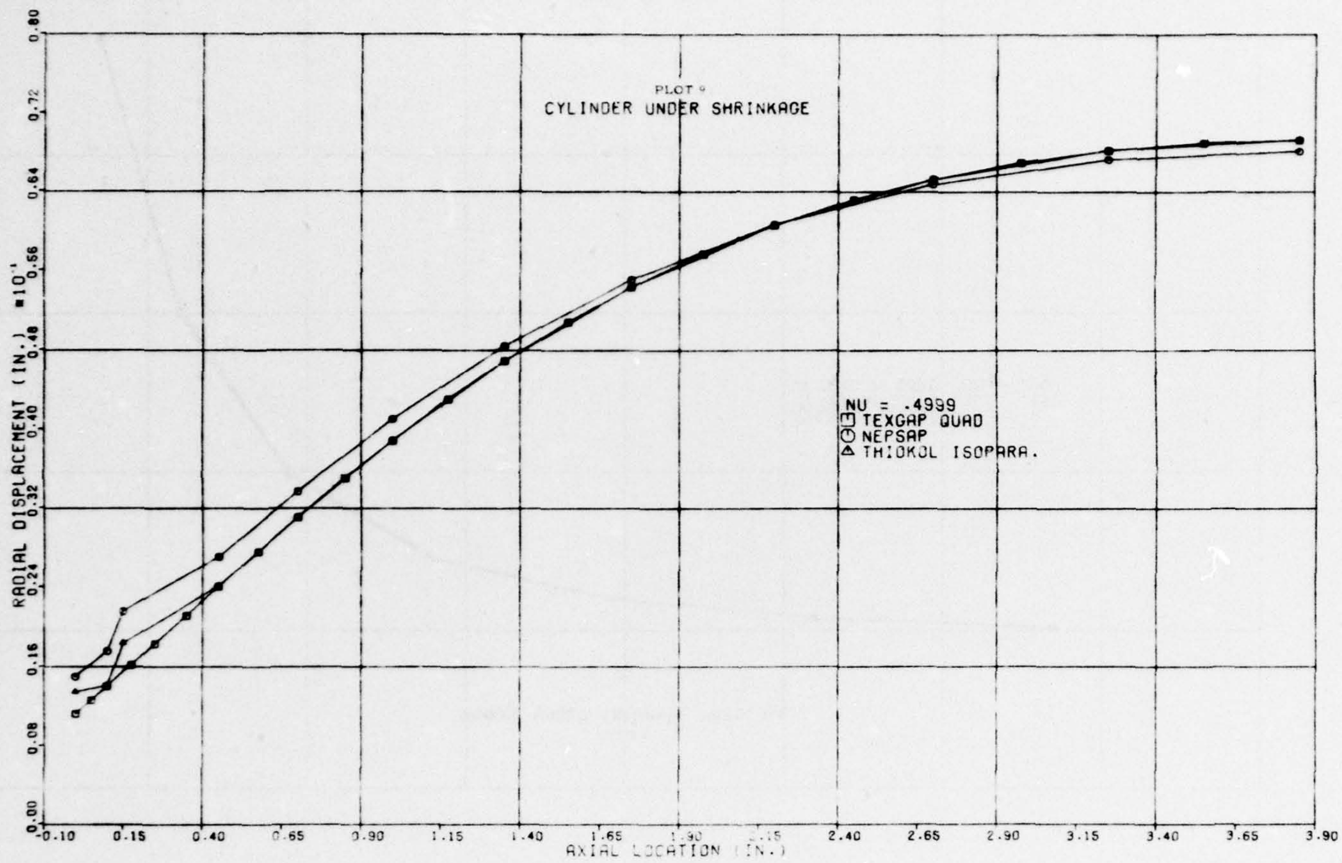

Figure A-9. Radial Displacement Vs Axial Location

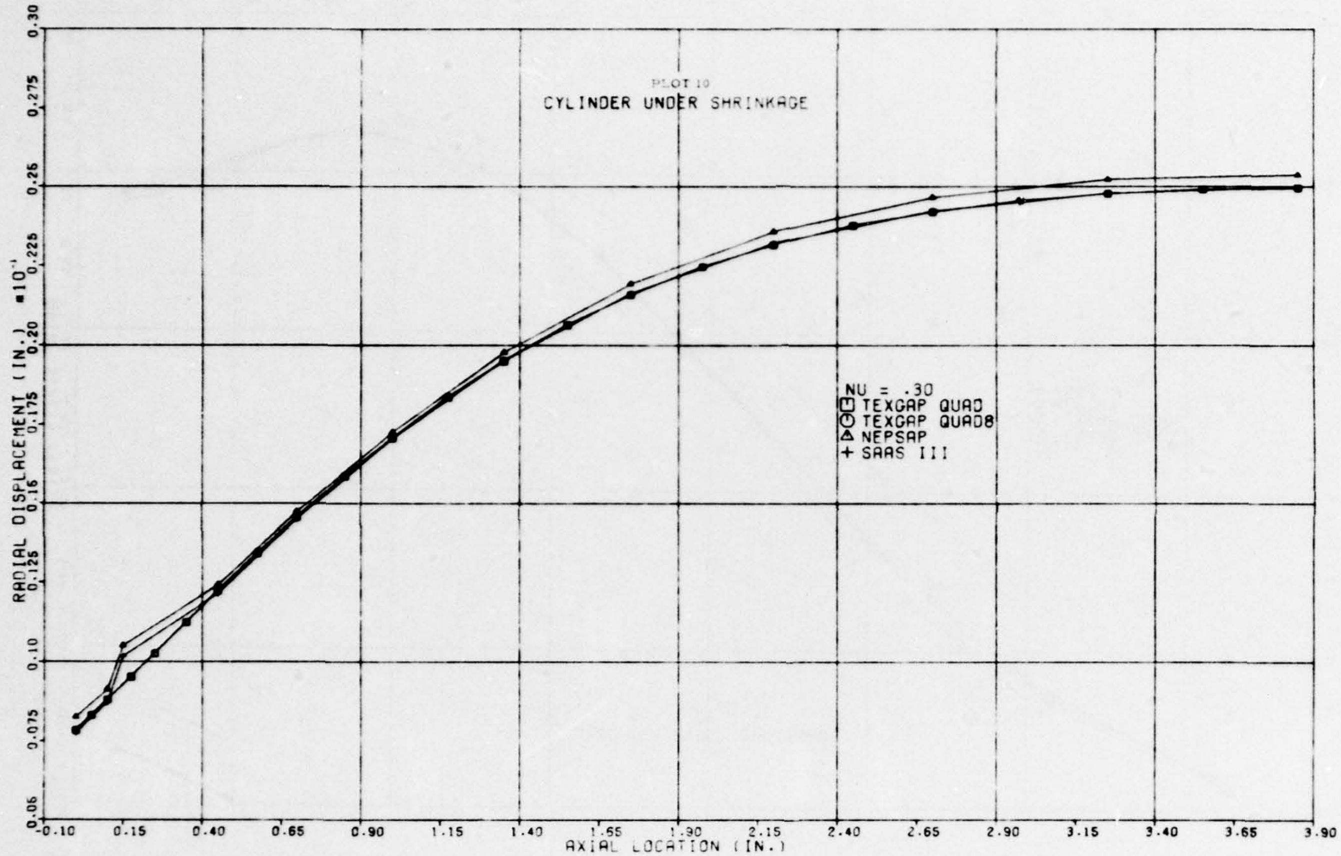

Figure A-10. Radial Displacement Vs Axial Location

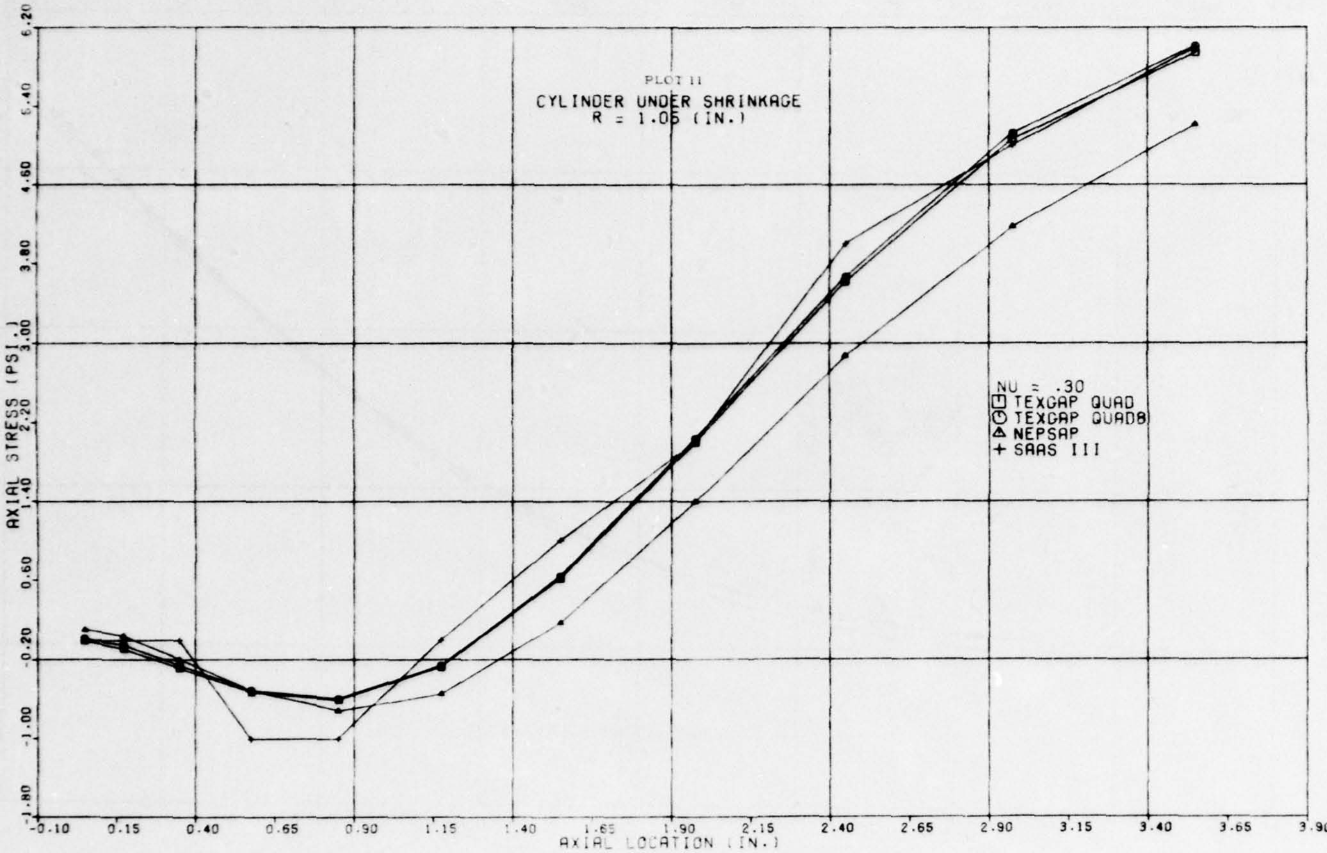

Figure A-11. Axial Stress Vs Axial Location

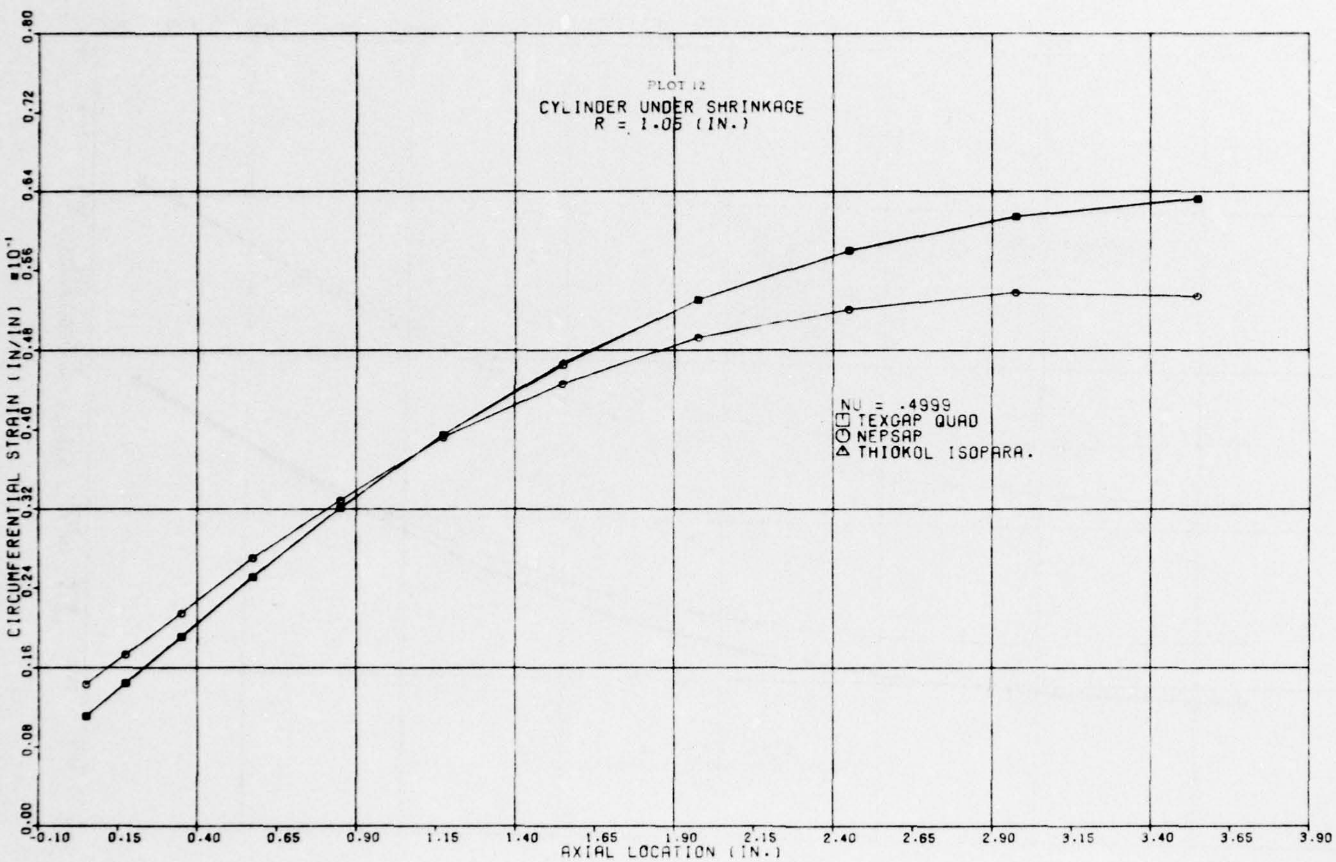

Figure A-12. Circumferential Strain Vs Axial Location

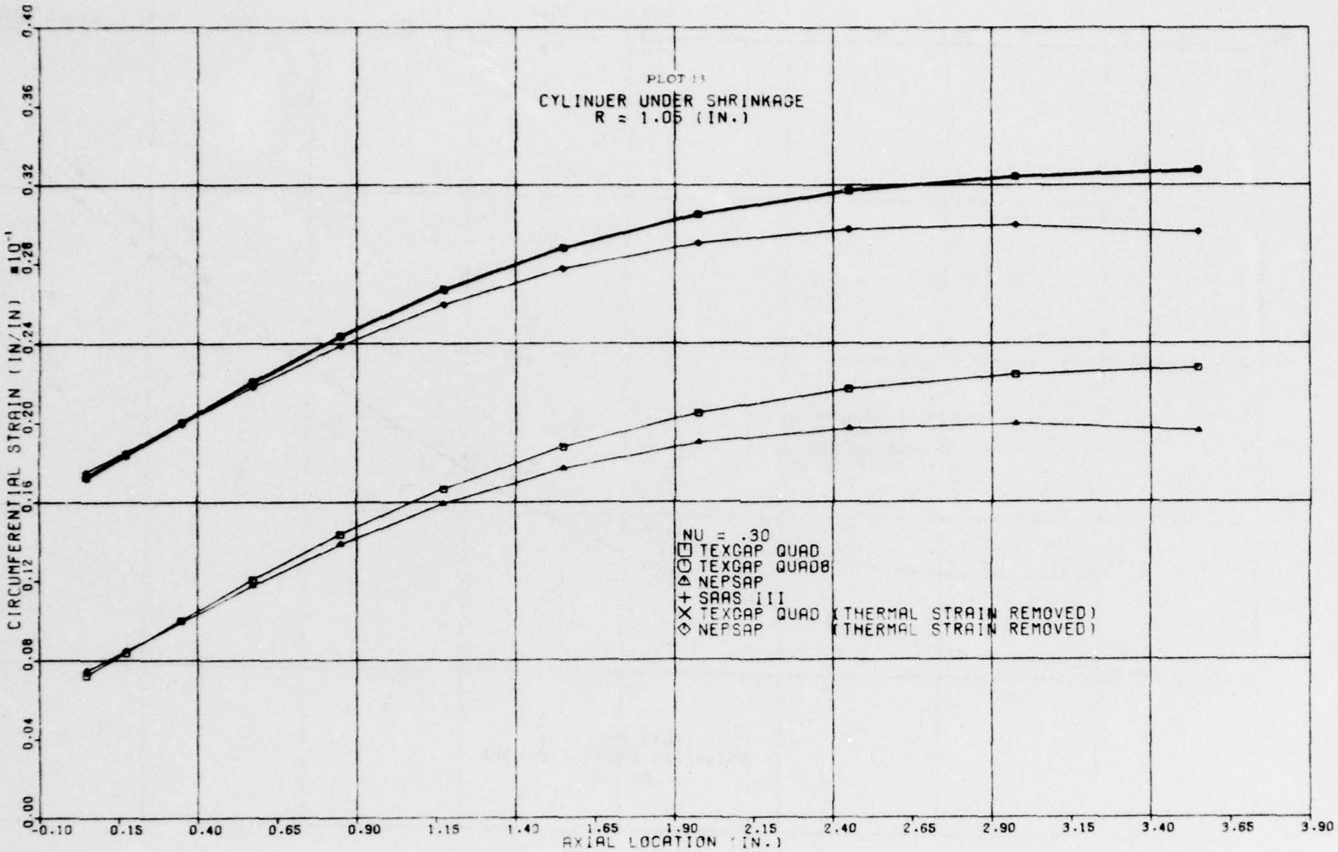

Figure A-13. Circumferential Strain Vs Axial Location

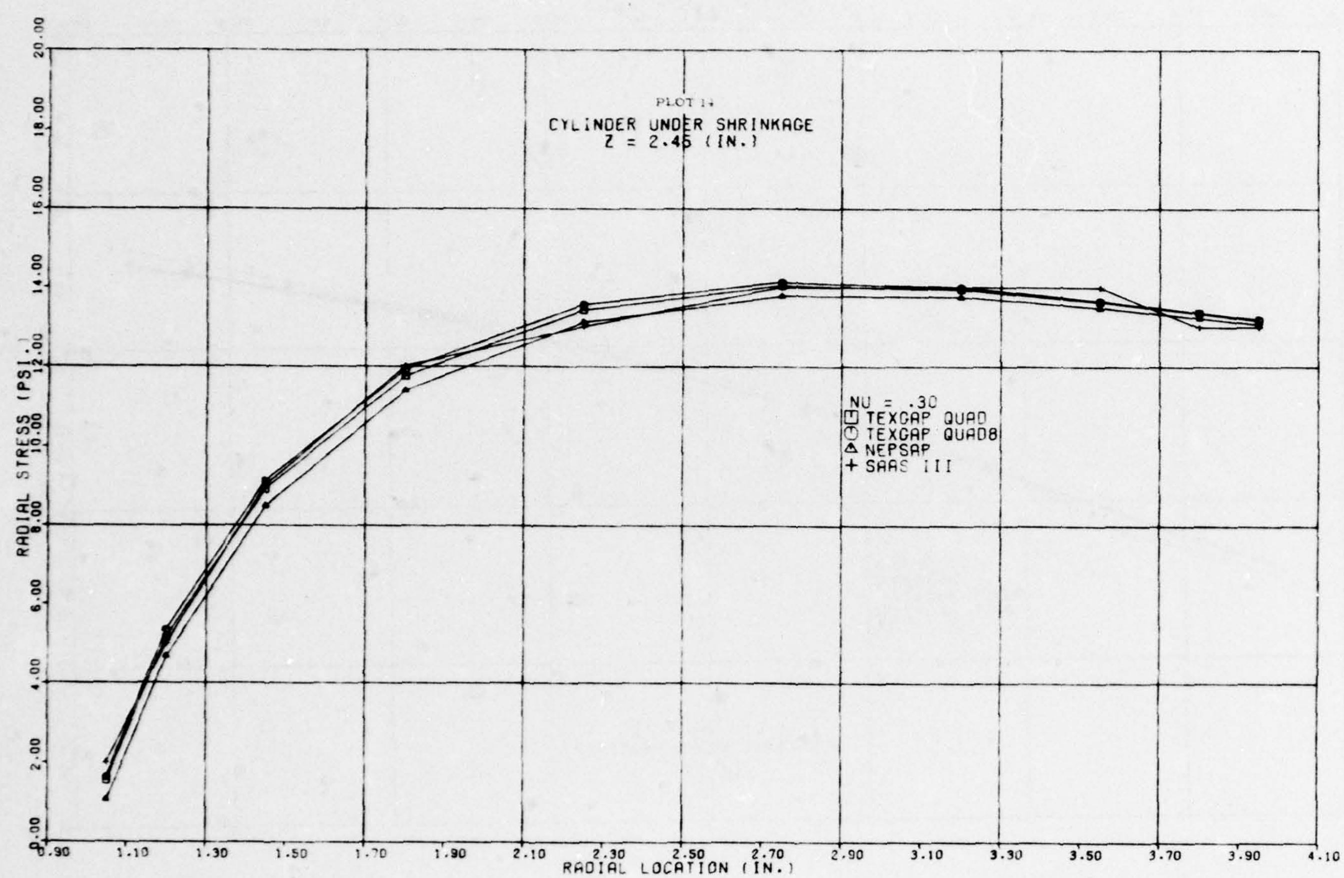

Figure A-14. Radial Stress Vs Radial Location

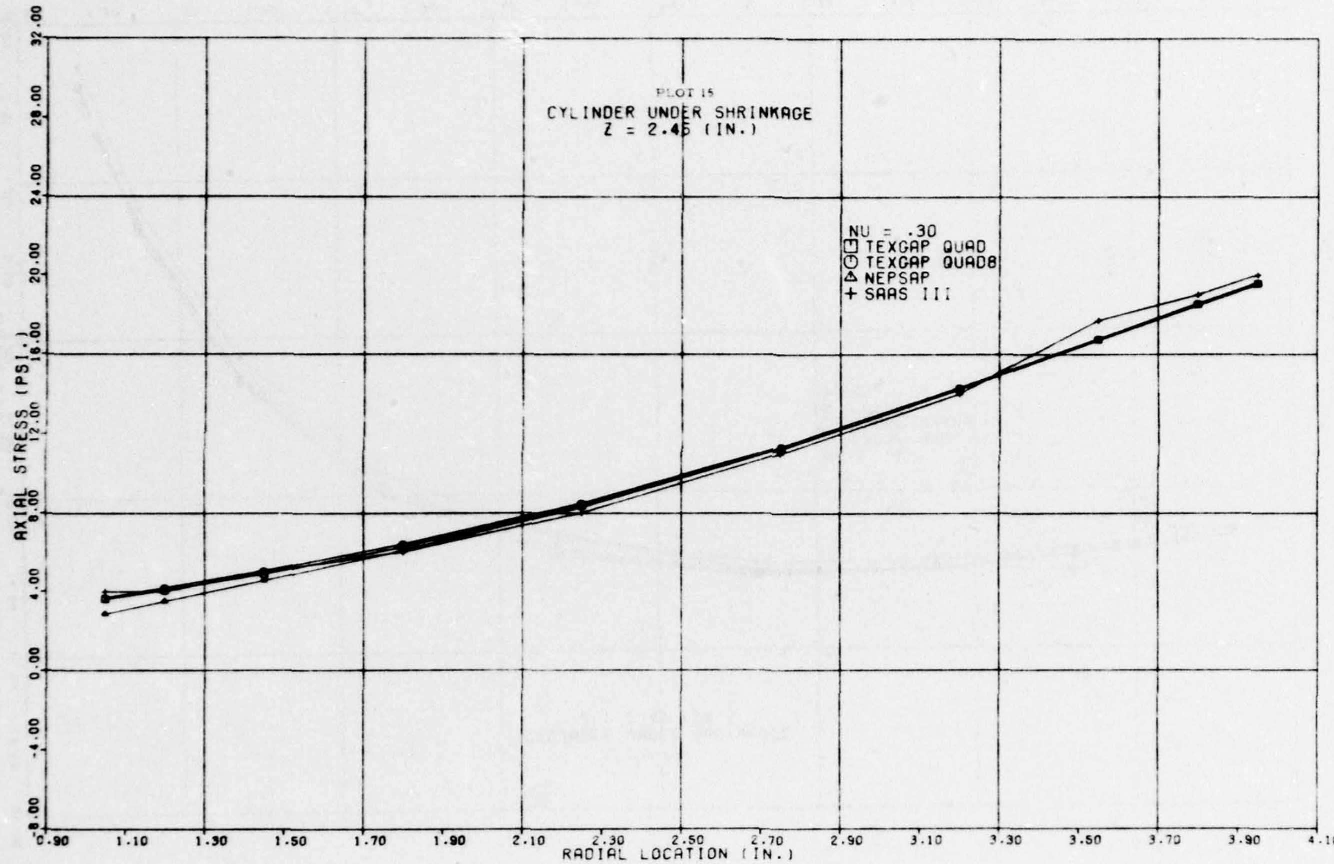

Figure A-15. Axial Stress Vs Radial Location

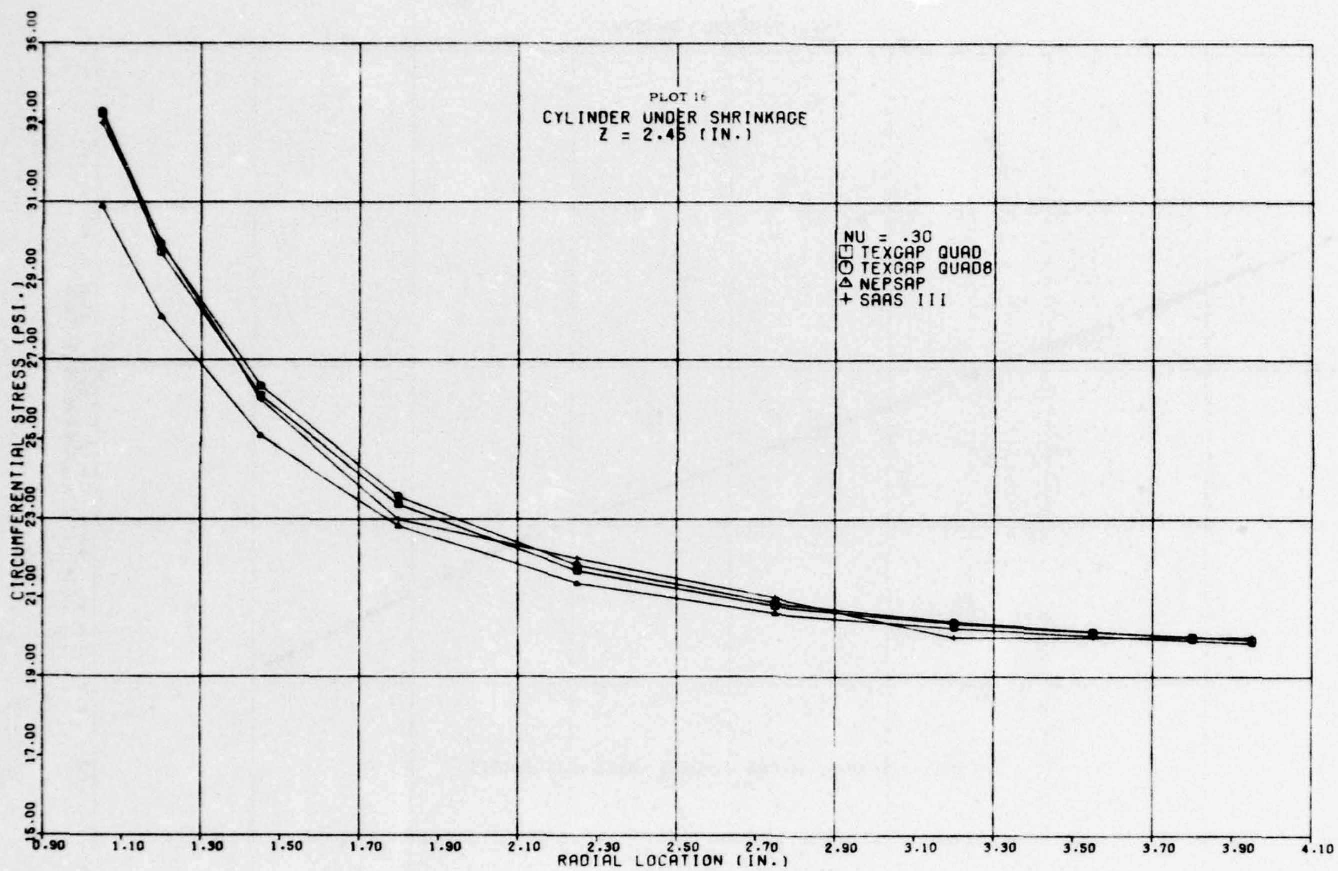

Figure A-16. Circumferential Stress Vs Radial Location

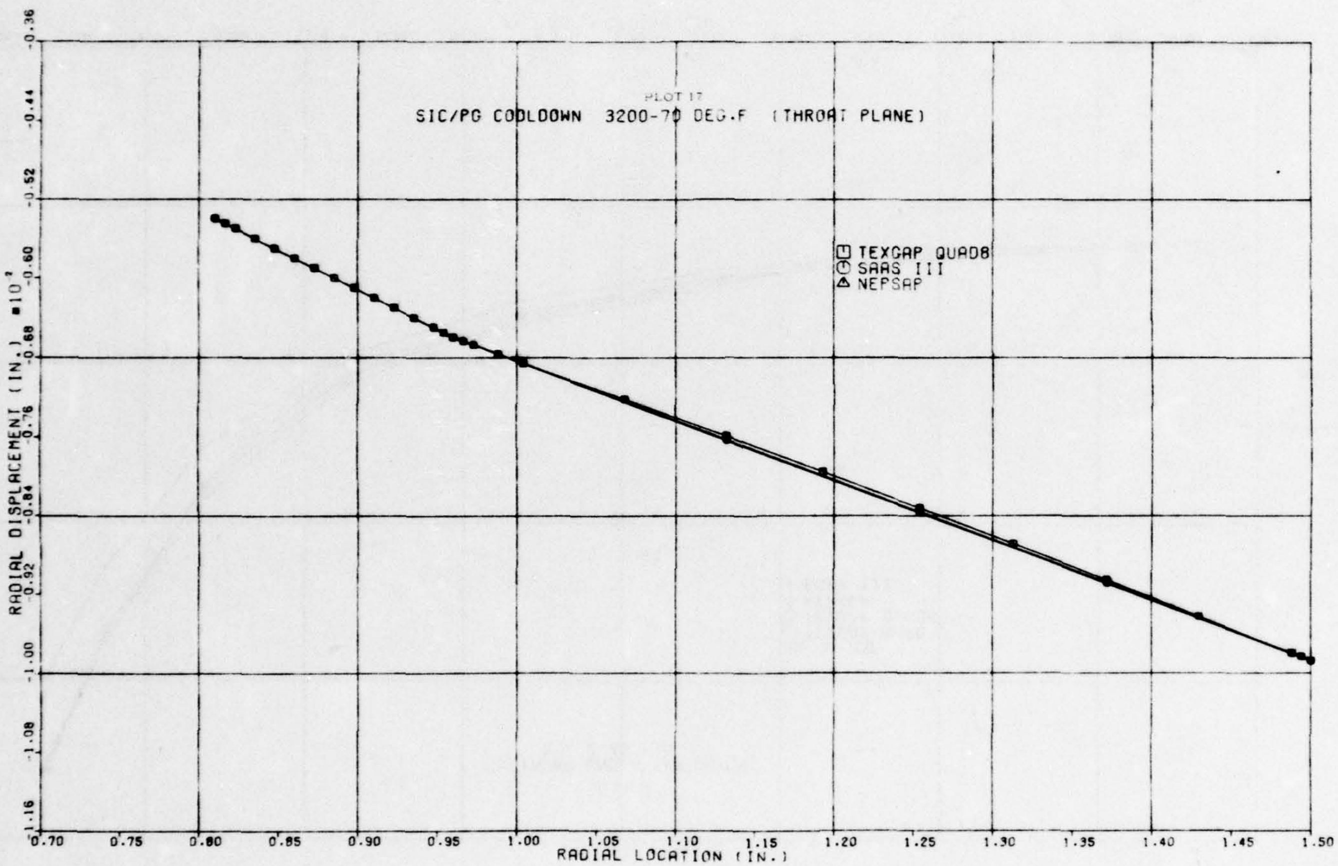

Figure A-17. Radial Displacement Vs Radial Location

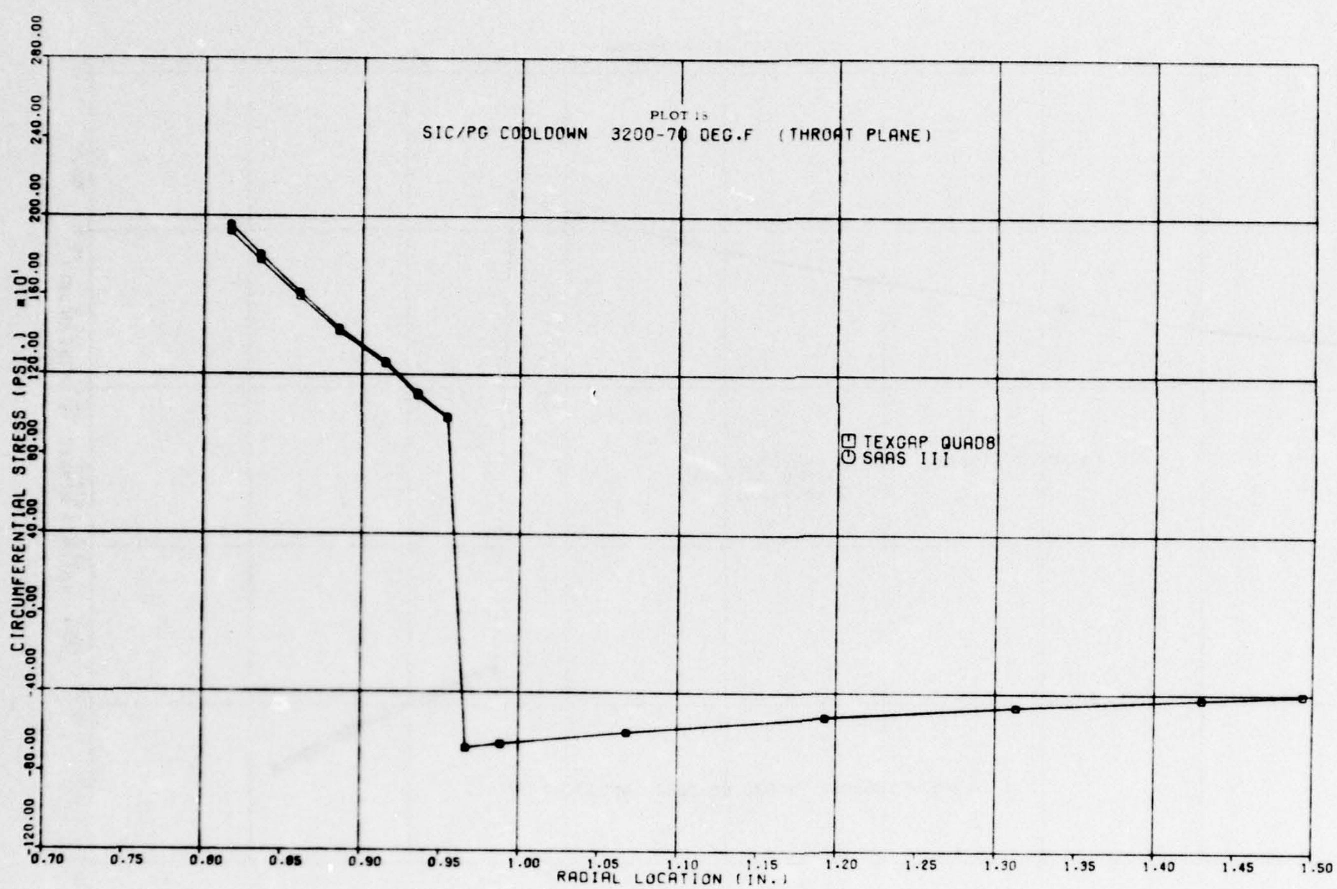

Figure A-18. Circumferential Stress Vs Radial Location

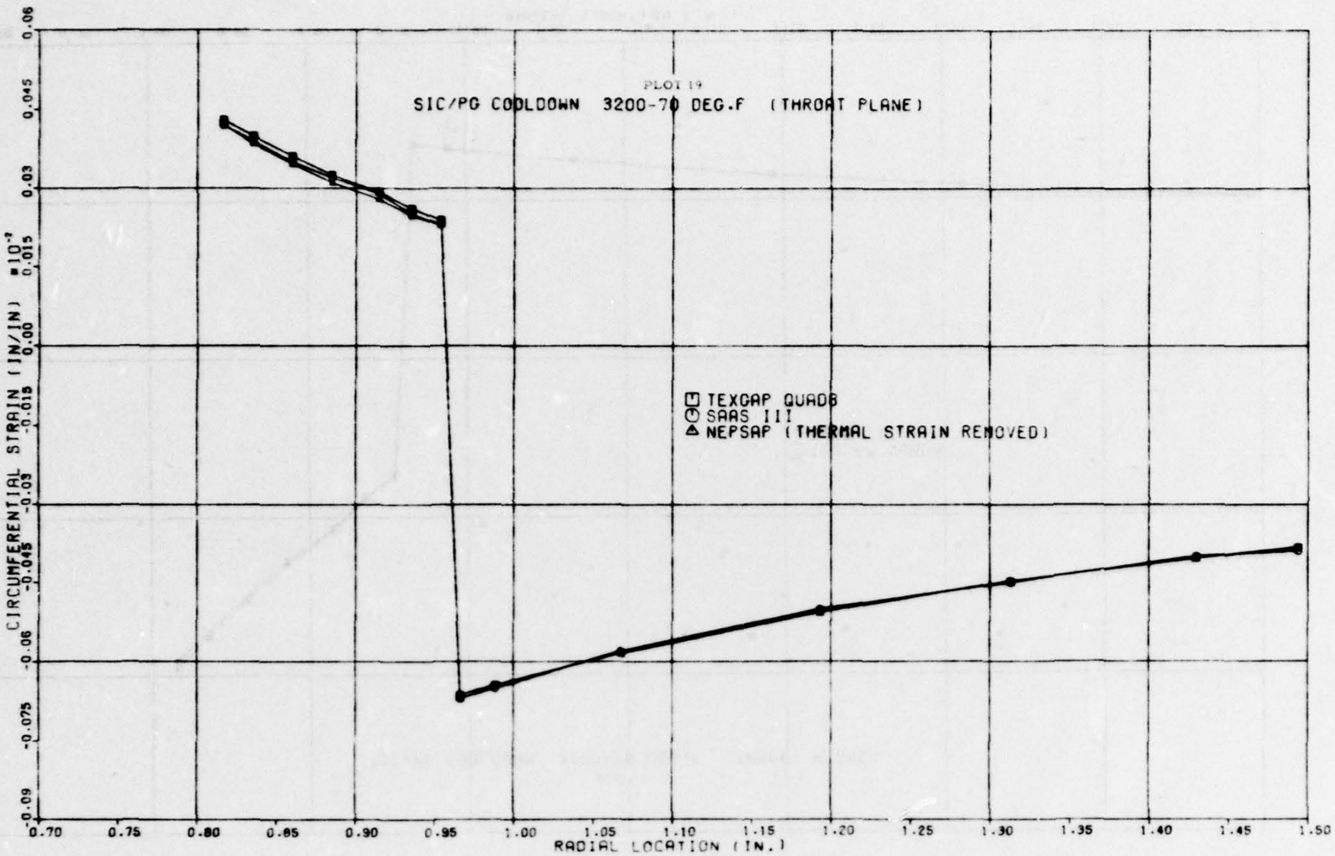

Figure A-19. Circumferential Strain Vs Radial Location